

Chapter IV

Results and discussions

4.1 Silicalite synthesis and characterization

The composition of the hydrogel formula of silicalite was $0.1\text{TPABr} \cdot 0.05\text{Na}_2\text{O} \cdot \text{SiO}_2 \cdot 80\text{H}_2\text{O}$ [6]. This experiment used Ludox and silica fumed for the source of silica. Both materials showed the same results of XRD patterns before calcination, Figures 4.1 and 4.2, which appear to match the standard pattern of silicalite, Figure 4.3. The TGA results of the silicalite from Ludox and silica fumed showed the temperatures at weight loss, which were $409\text{ }^\circ\text{C}$ and $408.2\text{ }^\circ\text{C}$, respectively. These results show the decomposition of the organic templates used in the synthesis. The TGA result from the use of Ludox, Figure 4.4, showed a better result than that from silica fumed, which exhibited some contaminants, Figure 4.5.

As mentioned, this hydrogel formula can be used to synthesize the silicalite. Ludox was selected for use as the source of silica for the preparation of the silicalite because the silicalite from Ludox had higher crystallinity than that from silica fumed. The suitable calcination temperature was $500\text{ }^\circ\text{C}$ because the TGA results showed that the organic templates would be removed from the silicalite under the temperature not lower than $410\text{ }^\circ\text{C}$.

4.2 The silicalite membrane on different supports

Silicalite membrane can be prepared on both silica fiber and porous borosilicate disc, as shown by the XRD patterns in Figures 4.6 and 4.7, which correspond to the standard XRD pattern of the silicalite. The SEM images of the silicalite membrane on both supports are shown in Figures 4.8 and 4.9. The crystal size of silicalite on silica fiber is approximately $4\text{-}6\text{ }\mu\text{m}$. However, the crystals did not cover all of the surface. On the porous borosilicate disc, the silicalite crystals formed over all the surface of the support. In addition, the silicalite crystals formed on silica

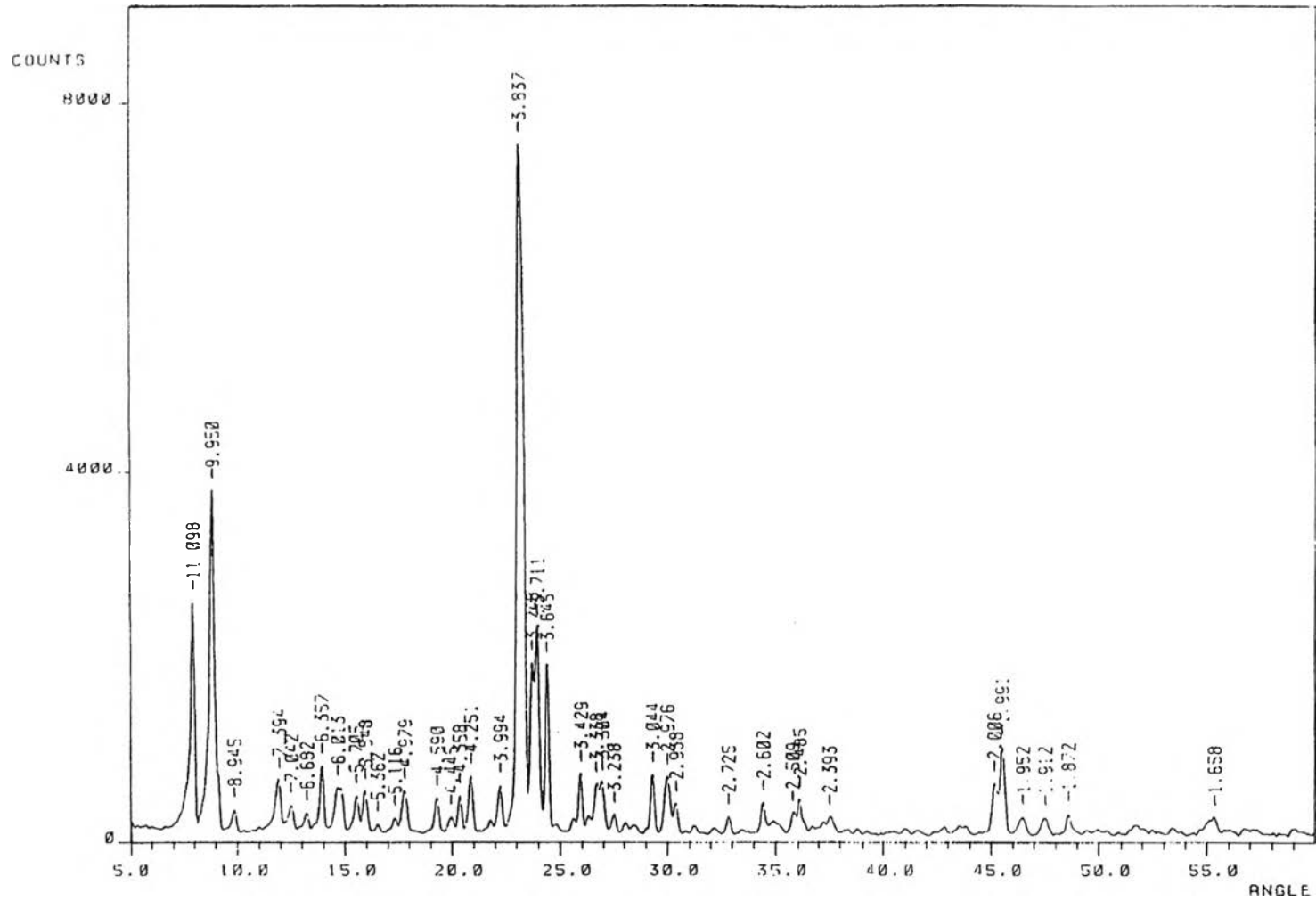


Figure 4.1 XRD pattern of the silicalite from Ludox before calcination.

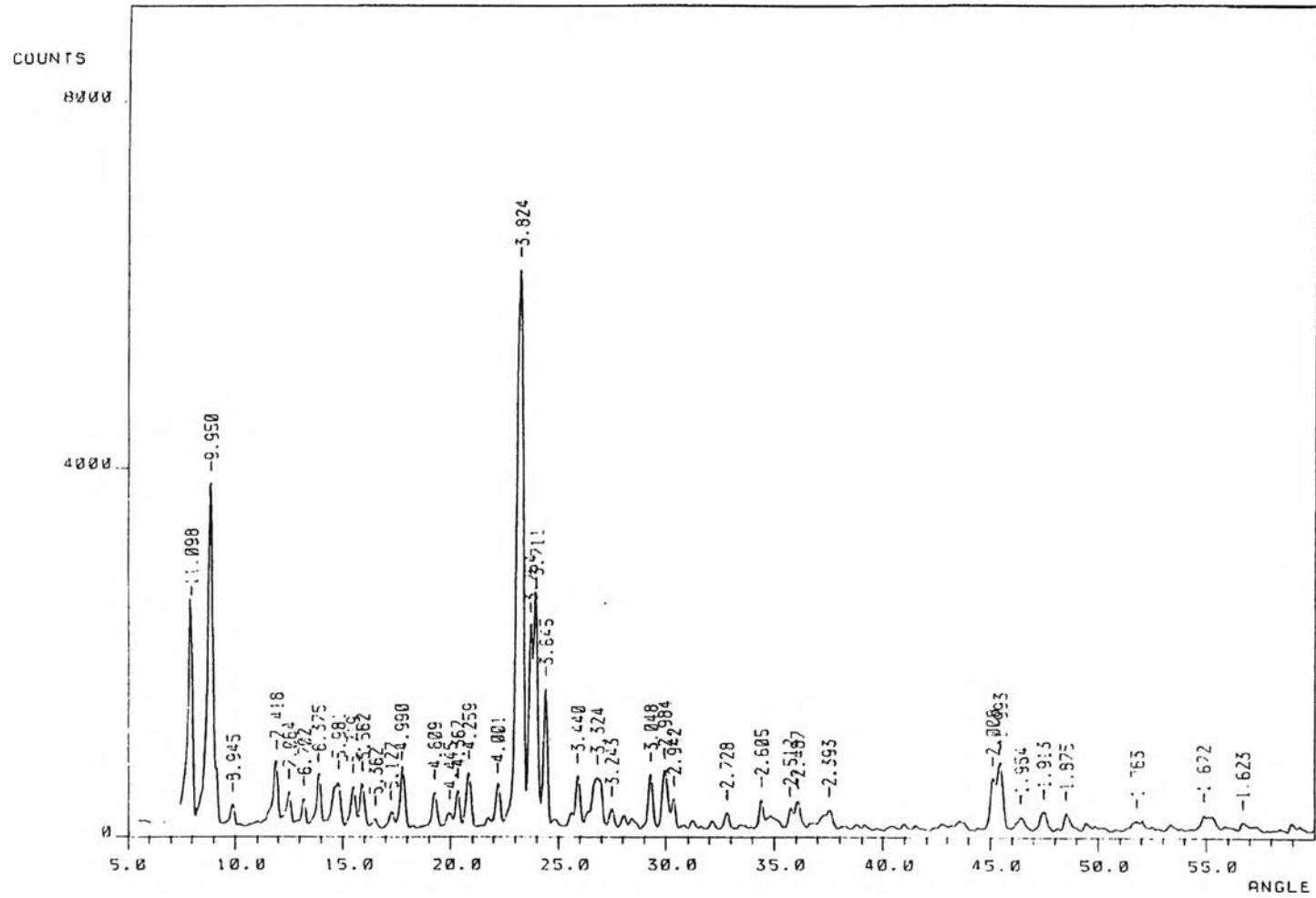


Figure 4.2 XRD pattern of the silicalite from silica fumed before calcination.

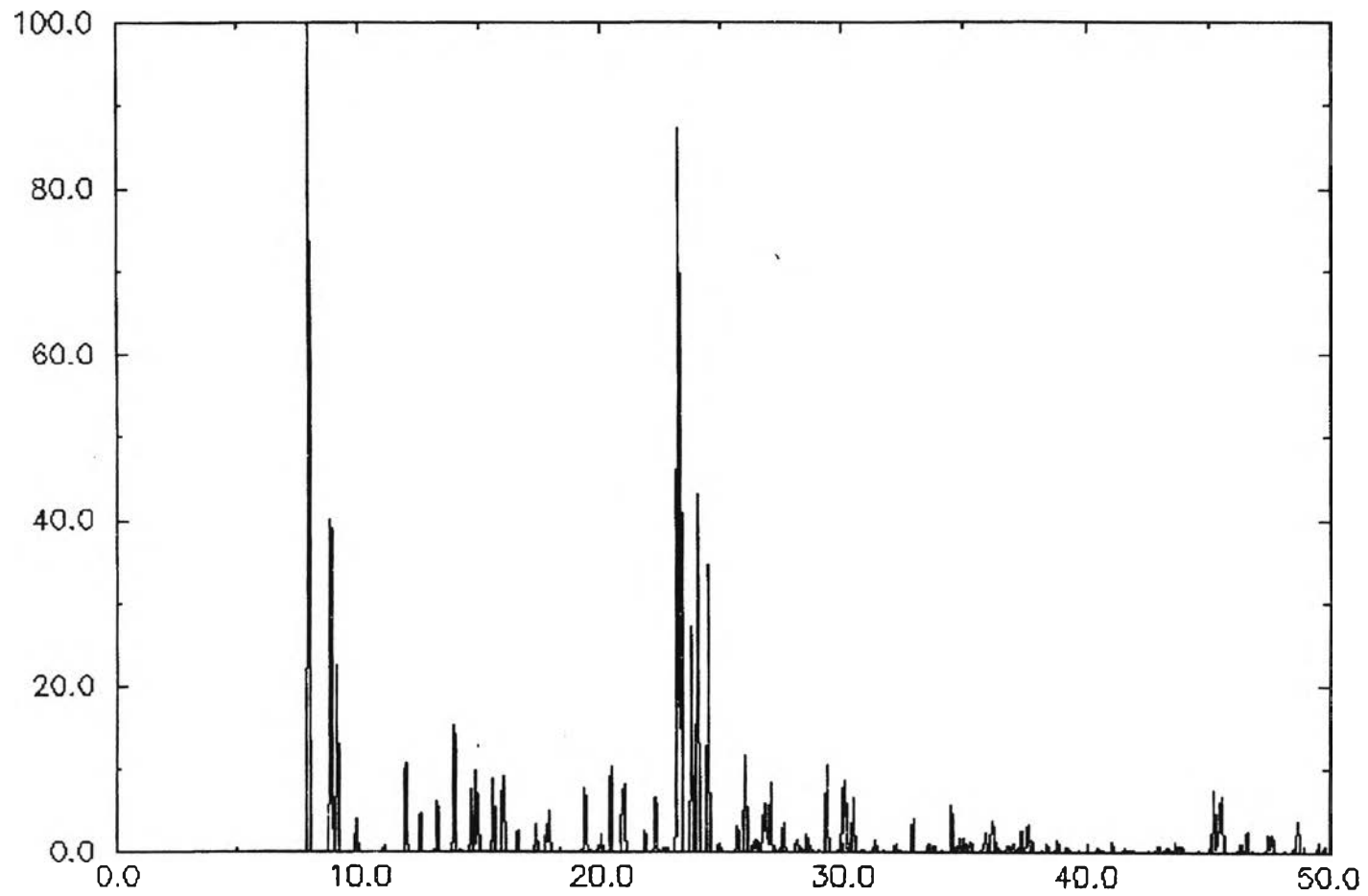


Figure 4.3 Standard XRD pattern of the silicalite before calcination [24].

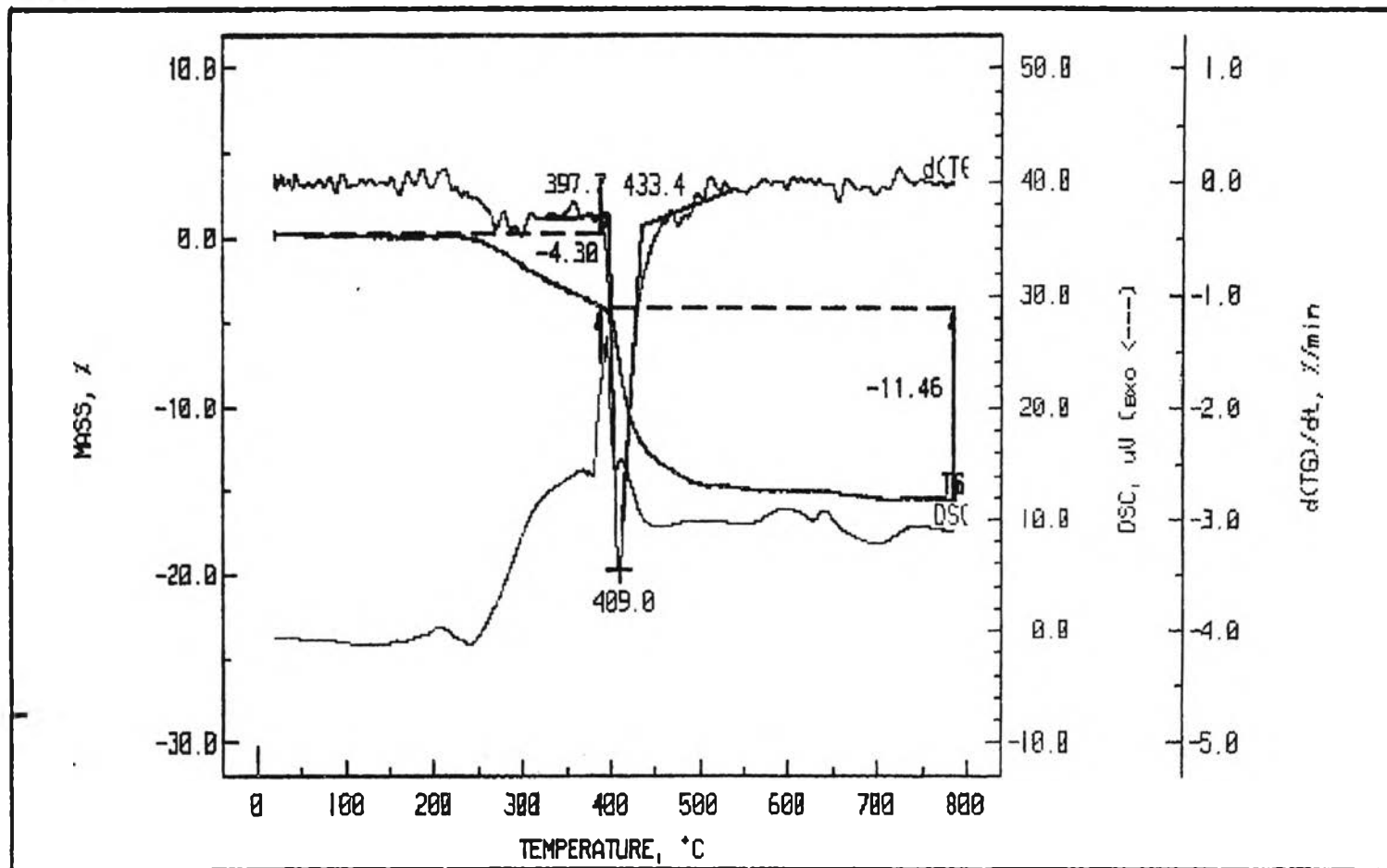


Figure 4.4 TGA thermogram of the silicalite from Ludox.

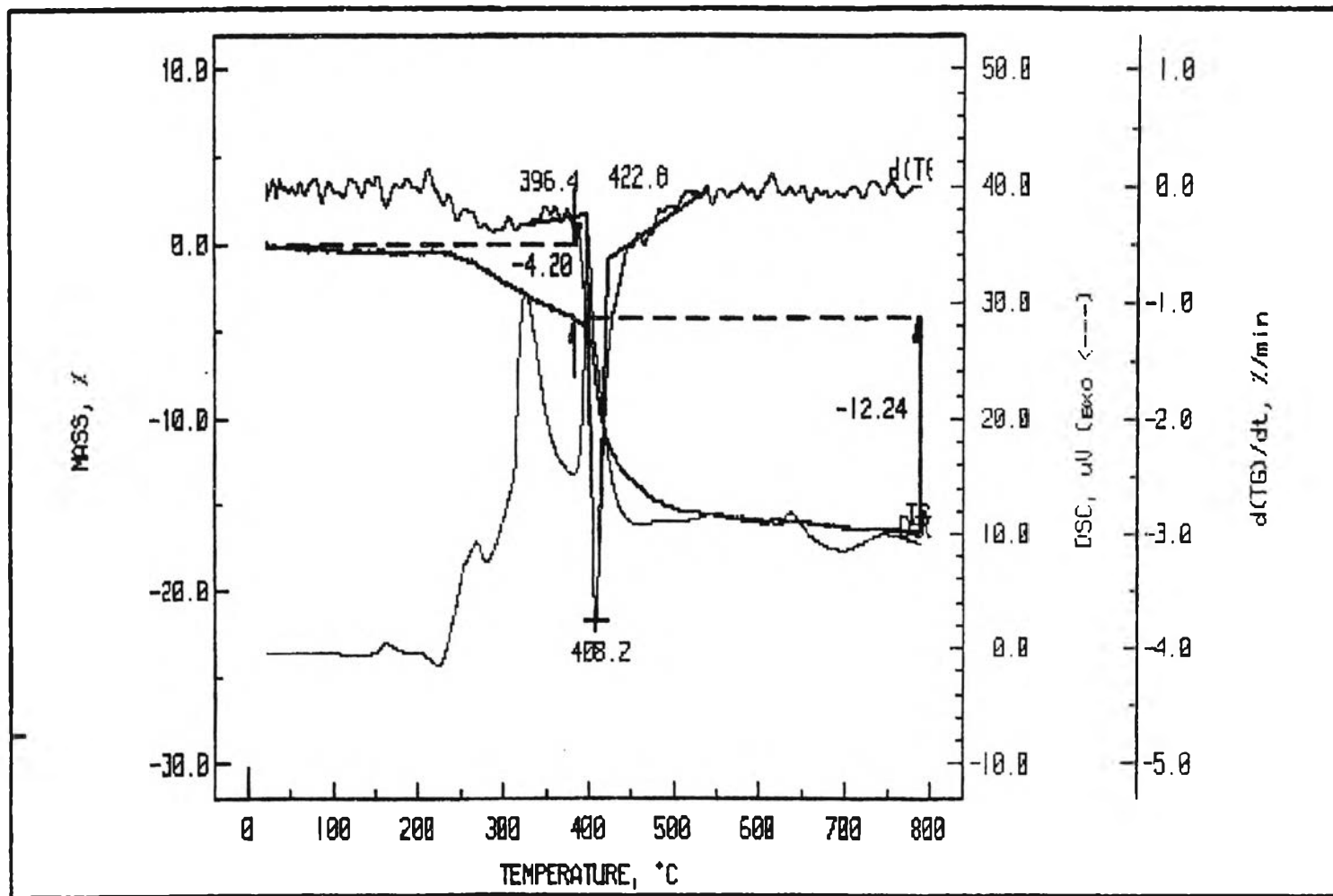


Figure 4.5 TGA thermogram of the silicalite from silica fumed.

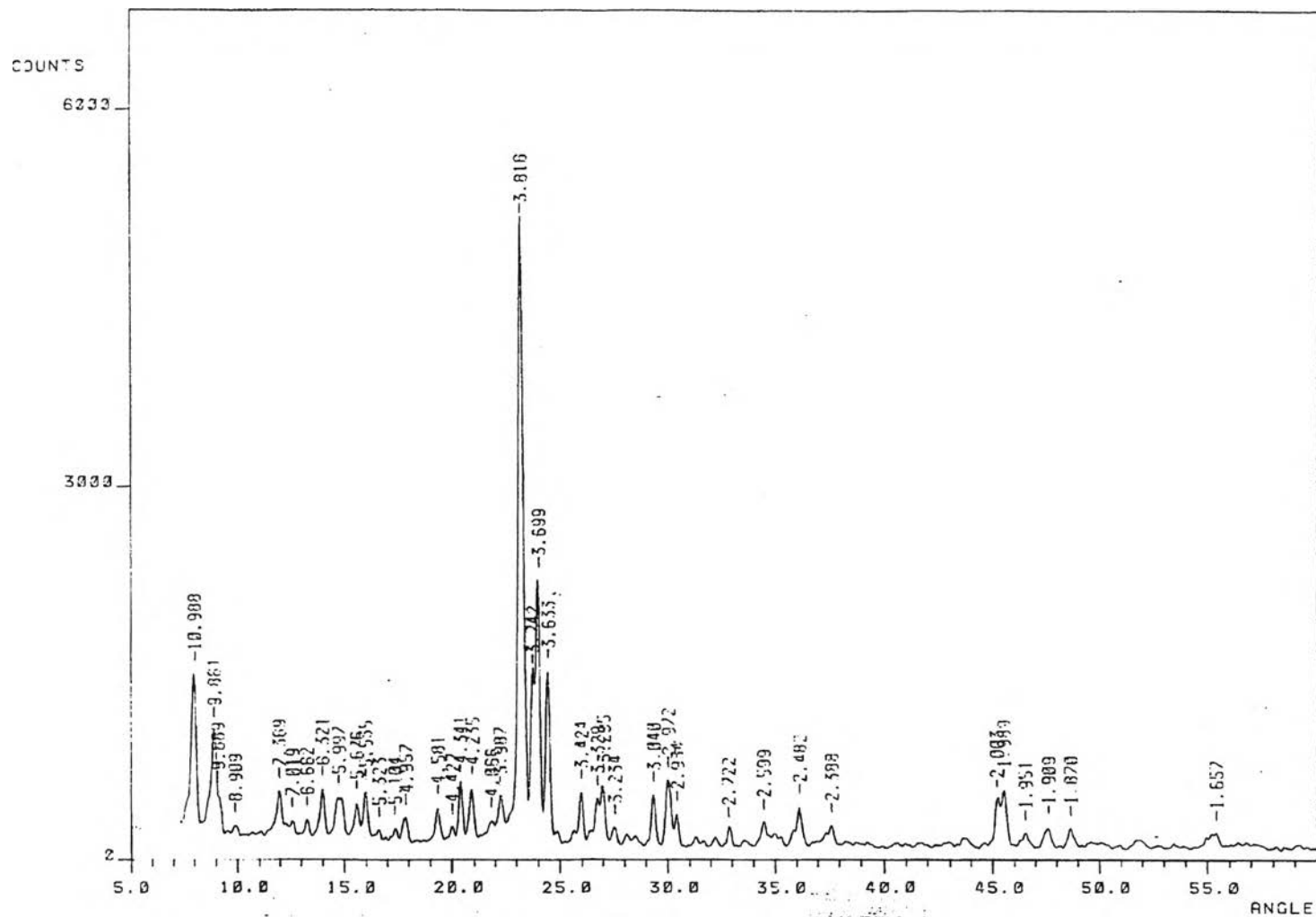


Figure 4.6 XRD pattern of silicalite membrane on silica fiber support.

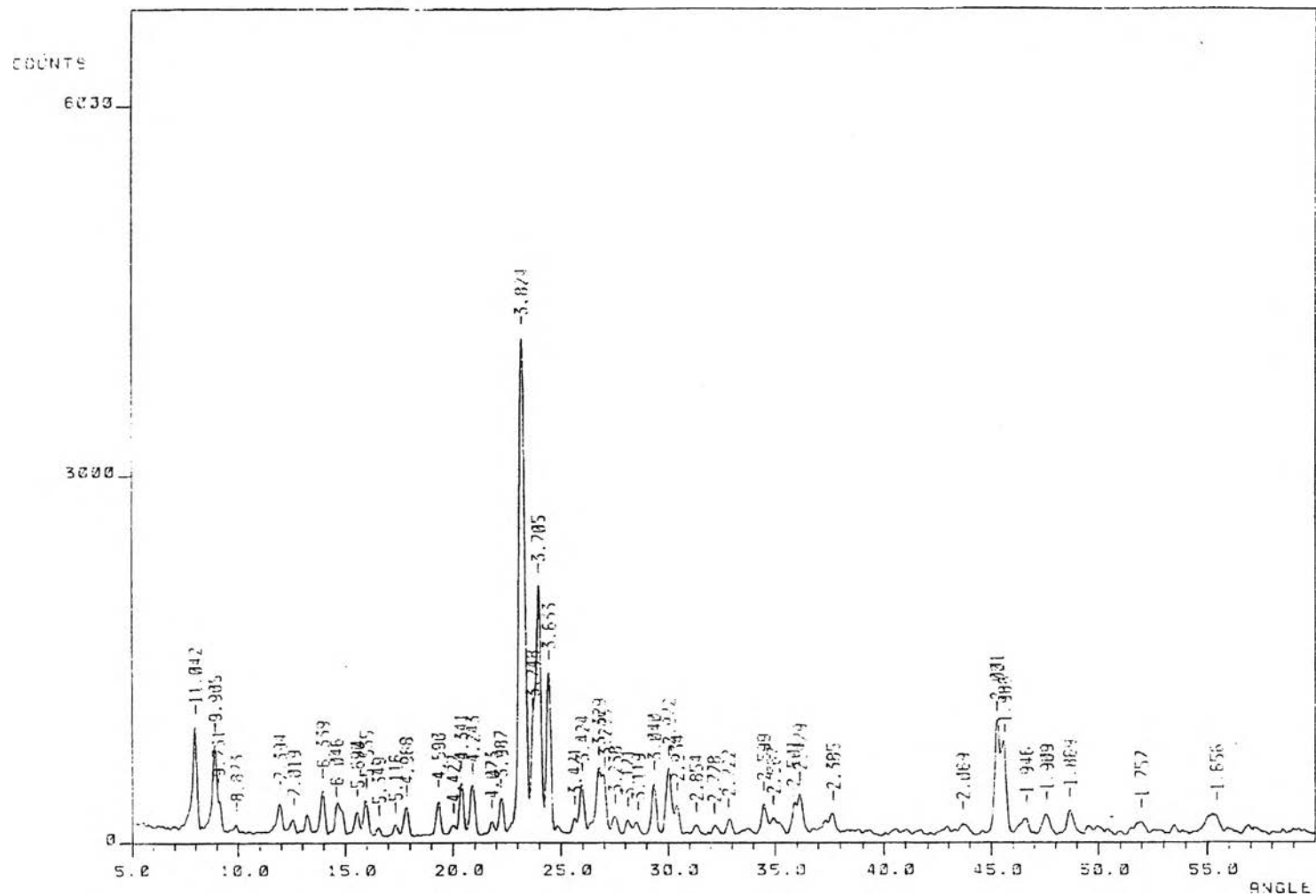


Figure 4.7 XRD pattern of silicalite membrane on borosilicate disc support.

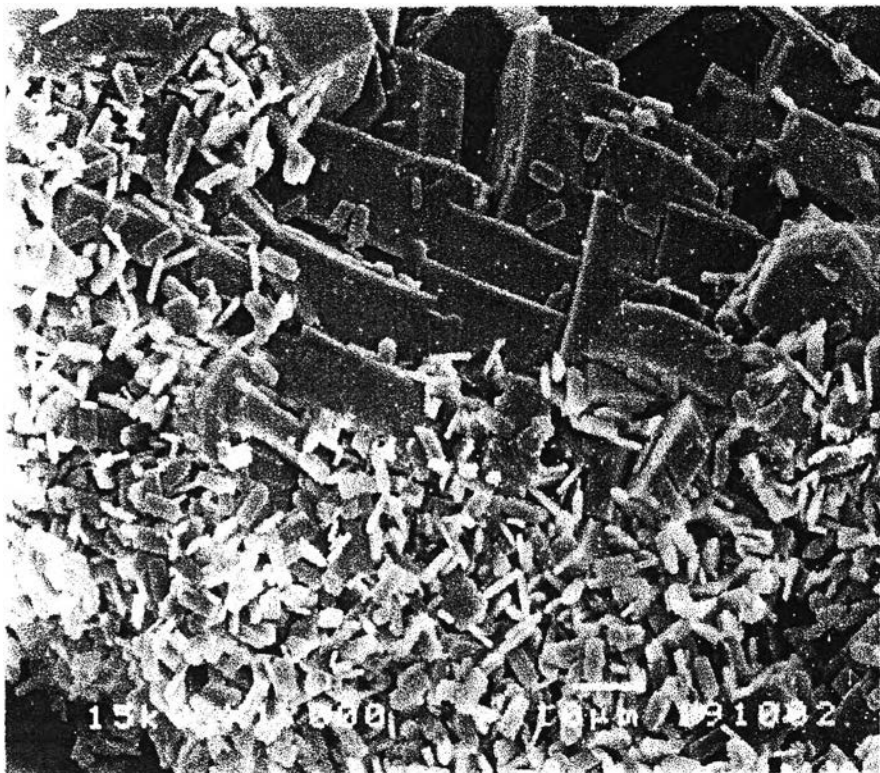


Figure 4.8 SEM image of silicalite membrane on silica fiber support.



Figure 4.9 SEM image of silicalite membrane on borosilicate disc support.

fiber support can be easily cracked but those on borosilicate disc supports are relatively strong.

The supports are different in types of materials, morphology and physical structure. Apparently, the porous borosilicate disc surface was smoother than the surface of silica fiber support. In fact, borosilicate disc support is more porous than silica fiber. In addition, the smooth surface of porous borosilicate disc facilitates crystal growth. Consequently, the porous borosilicate disc support was used in these experiments.

4.3 Silicalite membrane synthesis and characterization

4.3.1 The effect of support treatment

Figures 4.10 and 4.11 show the SEM images of silicalite membranes which were prepared using the above hydrogel formula on borosilicate disc supports with pore sizes 16-40 μm . with and without support treatment, respectively. The XRD patterns of these silicalite membranes are shown in Figures 4.12 and 4.13.

It can be seen that the silicalite membrane formed completely over the surface of the treated support. Whereas, on the untreated support, the surface was not completely covered by the silicalite membrane. Additionally, the crystallinity of silicalite membrane on the treated support is higher than the silicalite membrane formed on the untreated support. This can be attributed to the fact that contaminants, inside the pores and on the surface of the support, can be removed effectively by pretreatment which facilitates better nucleation and crystallization on the surface. Consequently, the support treatment is necessary for the membrane preparation. Therefore, in the experiments, all supports were treated before preparation of the silicalite membrane.

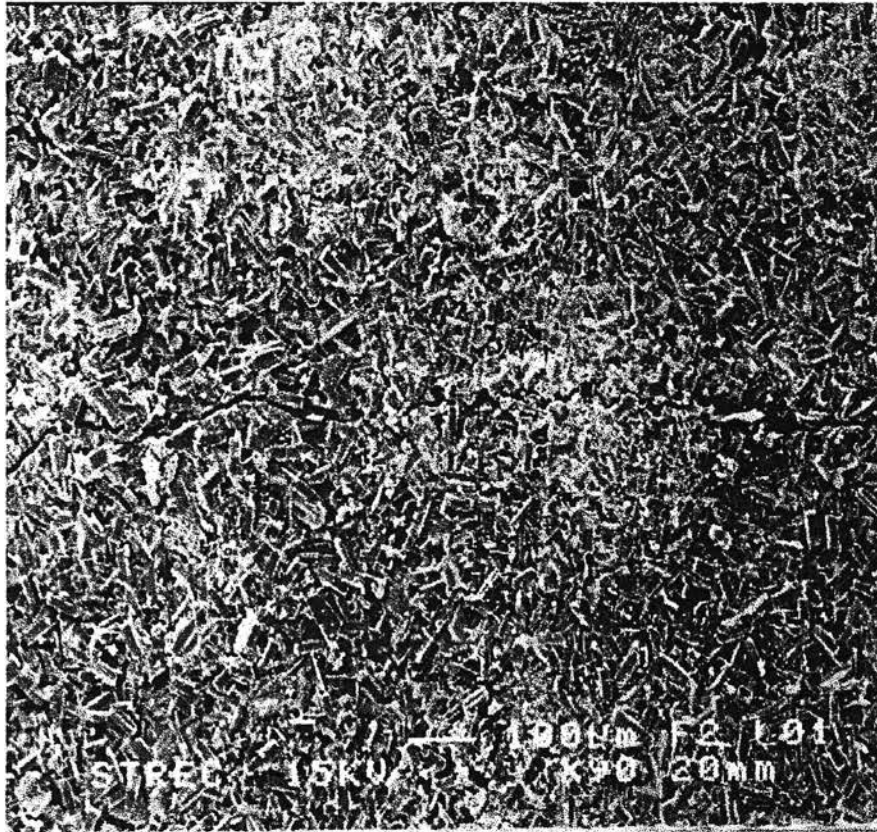


Figure 4.10 SEM image of silicalite membrane on treated borosilicate disc support.

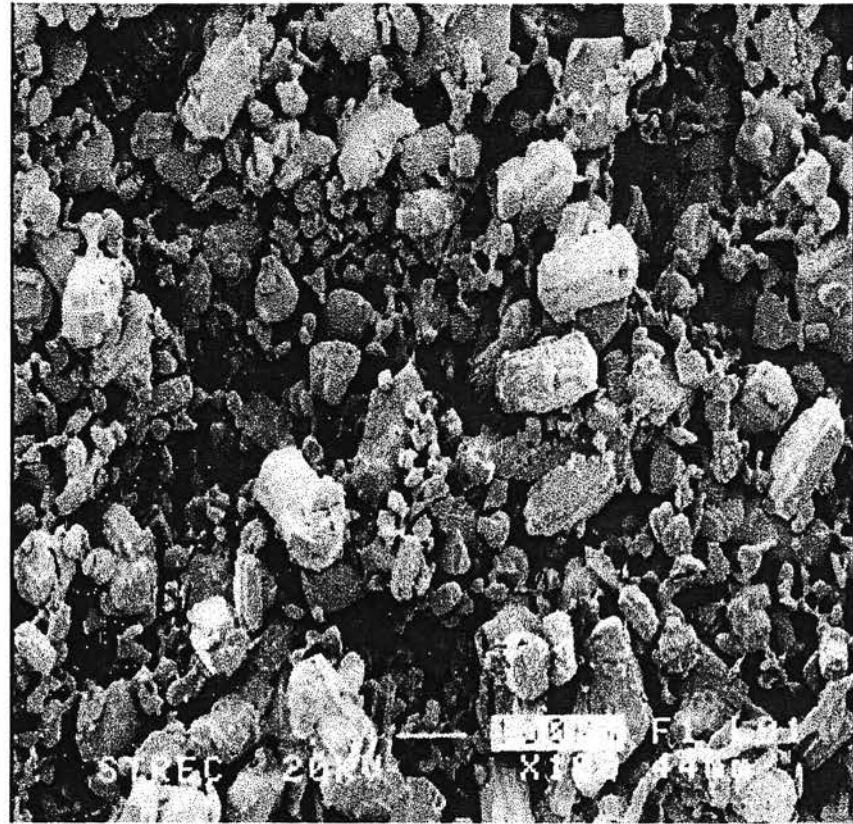


Figure 4.11 SEM image of silicalite membrane on untreated borosilicate disc support.

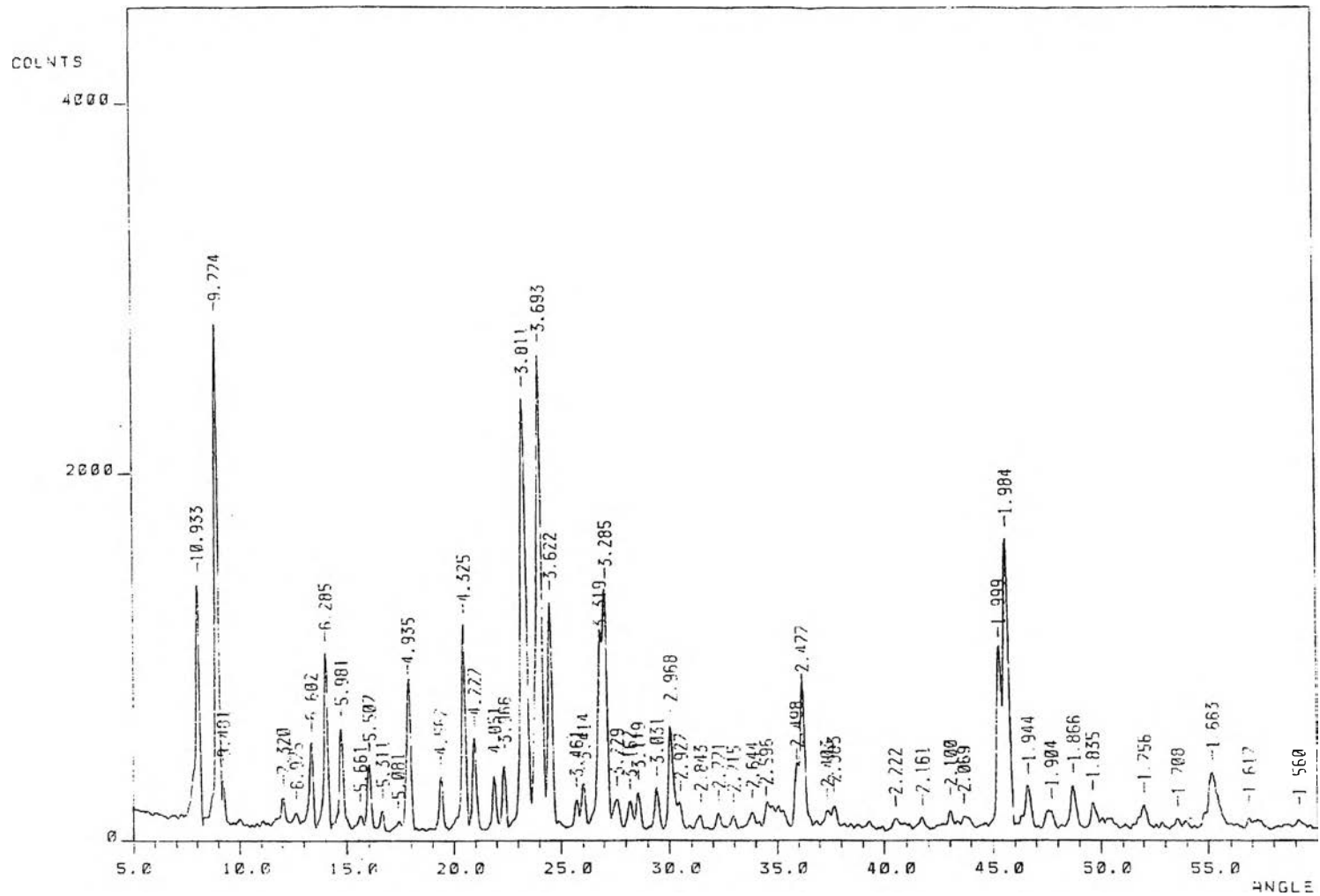


Figure 4.12 XRD pattern of silicalite membrane on treated borosilicate disc support.

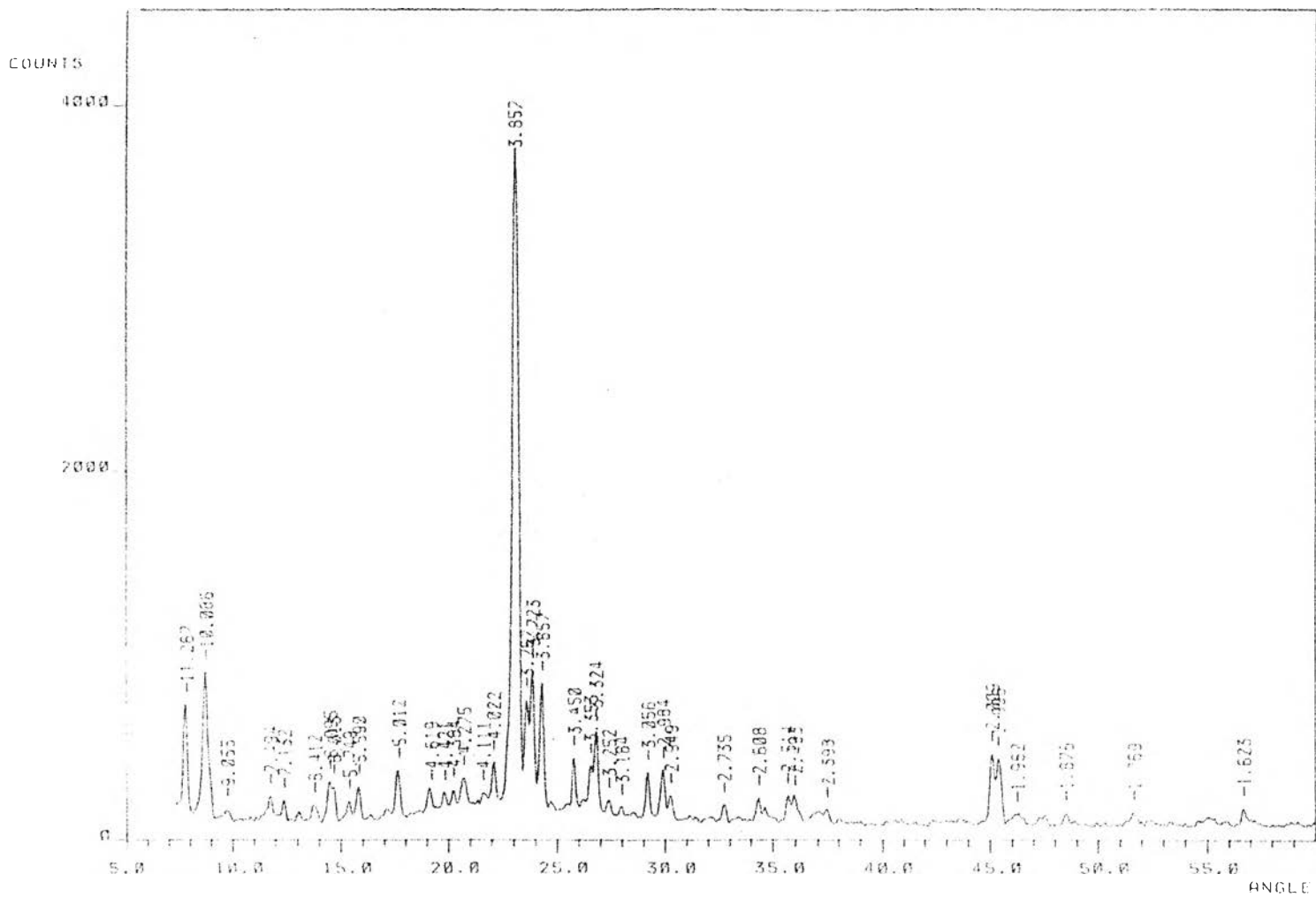


Figure 4.13 XRD pattern of silicalite membrane on untreated borosilicate disc support.

4.3.2 Calcination

Figure 4.14 shows the XRD patterns of silicalite membranes, before and after calcination. It was found that the templates remaining inside the pores of silicalite crystals were completely removed by calcination at 500 °C for 6 hours. Figure 4.14 (B) shows the XRD pattern of silicalite membrane after calcination which was almost the same as the standard pattern of silicalite, Figure 4.15. Therefore, this result confirms that the membrane formed on the porous borosilicate disc support was silicalite and the temperature used for calcination did not alter the crystal structure of the membrane.

4.3.3 The pore size effect of the borosilicate disc support

The borosilicate disc support was used with various pore sizes, 4-5.5 μm ., 10-16 μm ., and 16-40 μm .. The SEM images of the silicalite membranes of each support exhibited different crystal sizes and membrane thicknesses. The SEM images of cross sections of the silicalite membrane on the borosilicate support, pore sizes 4-5.5 μm ., 10-16 μm ., and 16-40 μm ., are shown in Figures 4.16, 4.17 and 4.18, respectively. The crystal sizes of silicalite and the thicknesses of silicalite membranes are shown in Table 4.1. Figure 4.19 shows a view of the cross section of a membrane at higher magnification. It was found that the support side consists of small silicalite crystals while crystal sizes in the middle of this support were relatively large and crystal sizes on the top layer were the largest.

Table 4.1 The crystal sizes of silicalite and the thicknesses of silicalite membranes on each support.

| Support No. | Pore sizes (μm .) | Crystal sizes of silicalite (μm .) | Thicknesses of silicalite membranes (μm .) |
|-------------|----------------------------------|---|---|
| 1 | 4-5.5 | 3-30 | 150 |
| 2 | 10-16 | 10-50 | 250-300 |
| 3 | 16-40 | 8-80 | 300 |

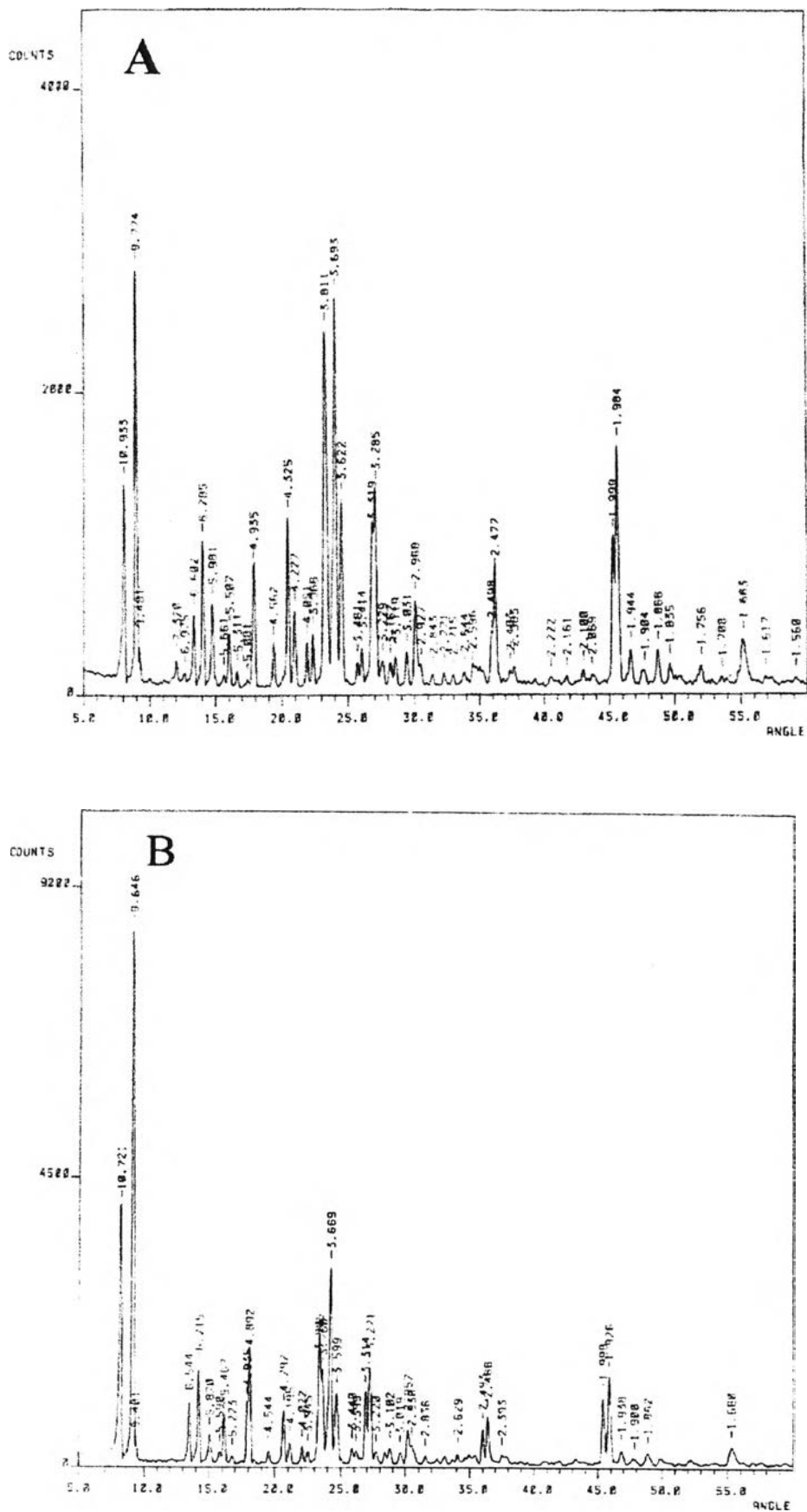


Figure 4.14 XRD patterns of silicalite membrane. A: before calcination; B: after calcination at 500 °C.

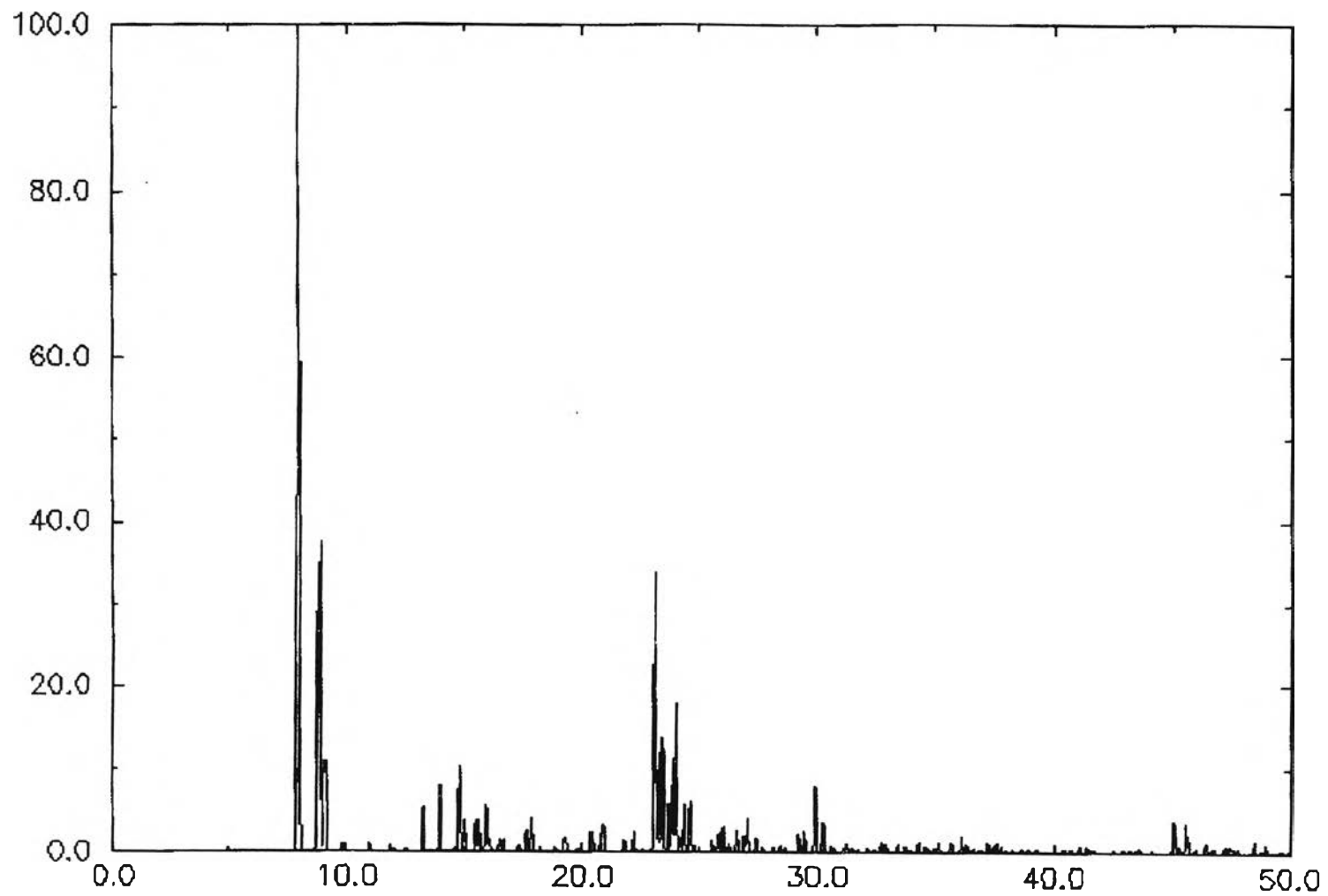


Figure 4.15 Standard XRD pattern of silicalite after calcination [24].

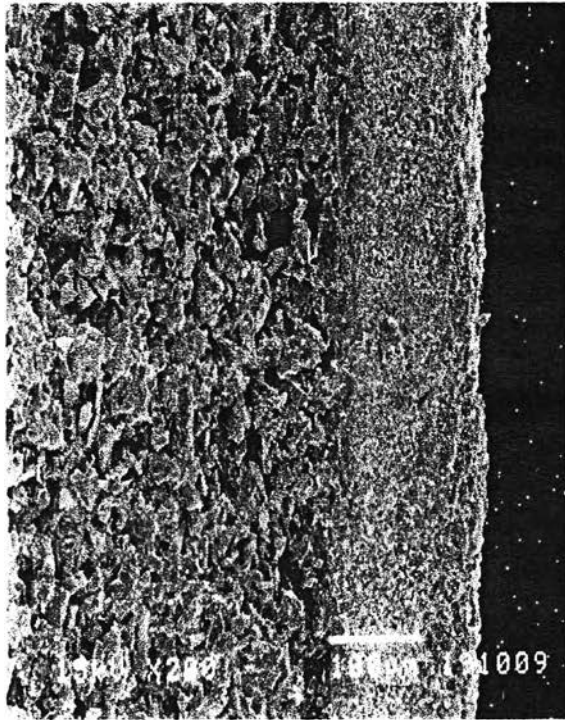


Figure 4.16 SEM image of cross section of silicalite membrane on the borosilicate disc support, 4-5.5 μm .

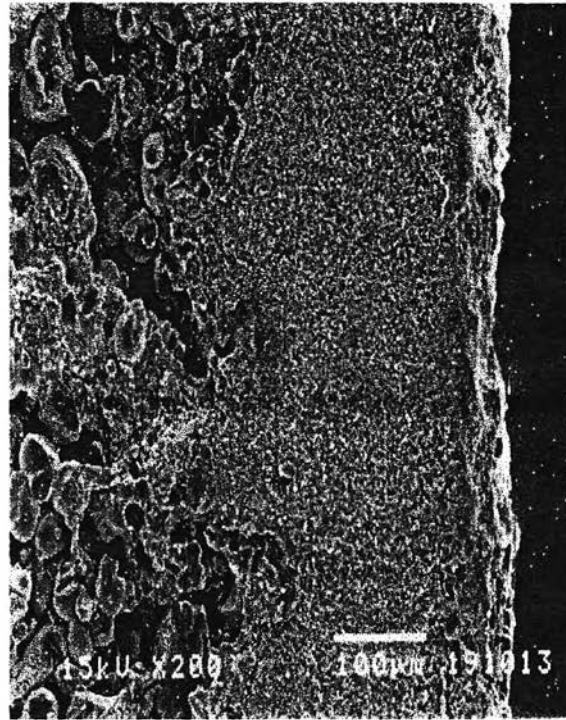


Figure 4.17 SEM image of cross section of silicalite membrane on the borosilicate disc support, 10-16 μm .

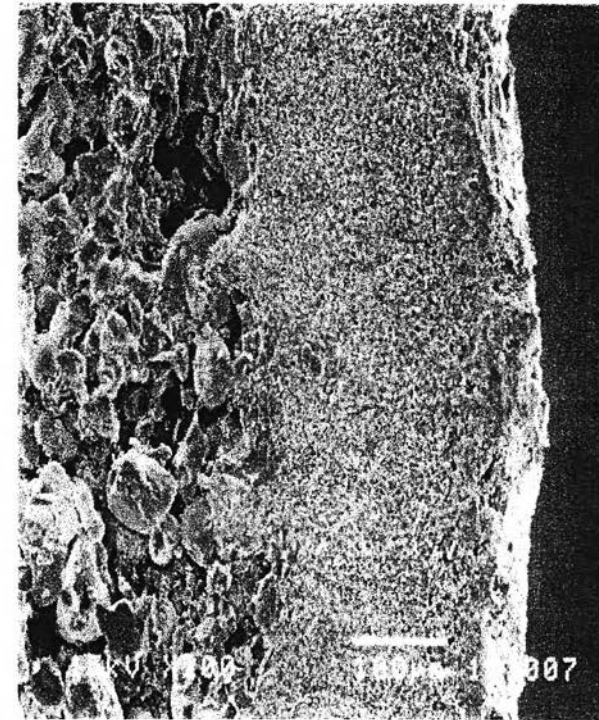


Figure 4.18 SEM image of cross section of silicalite membrane on the borosilicate disc support, 16-40 μm .

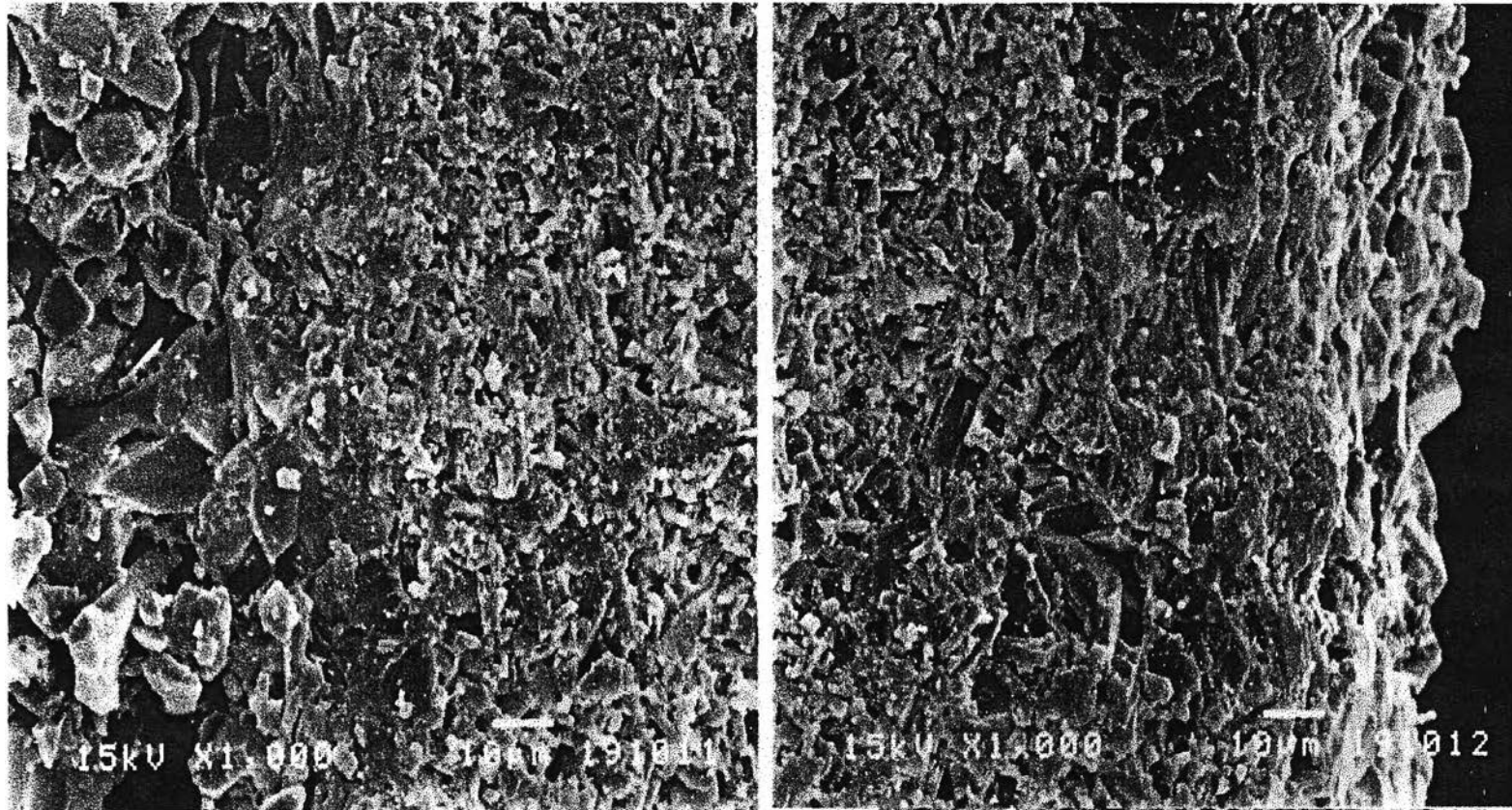


Figure 4.19 SEM image of cross section of silicalite membrane at higher magnification. A: the silicalite crystals at the support side, B: the silicalite crystals at top layer.

These observations confirm that the pore sizes of the borosilicate support effect the crystal size and the thickness of membrane. It was found that, under the same preparation conditions except the difference in pore sizes of support, the small pore sizes resulted in small crystals and the large pore sizes resulted in large crystals of silicalite membrane. This can be accounted from the fact that the crystal growth is a phase transformation from liquid to solid which relates to surface tension and nuclei [25]. Therefore, on supports with the same diameter, the support with the small pore sizes has a higher surface area than the support with a large pore sizes, and the small pore sizes generate higher surface tension than the large pore sizes. The high surface tension strongly effects rate of nucleation which results in large numbers of small nuclei. Consequently, the small silicalite crystals were formed on the support with small pore sizes.

4.4 Gas separation process

4.4.1 Sealing procedures

A support covered with silicalite membrane was sealed within 3-way Pyrex glass by either gas welding or epoxy resin. In case of gas welding, the silicalite membrane on the support and 3-way Pyrex glass was sealed at high temperature, Figure 3.2 (A). The cell was installed with the gas sampling line of GC as shown in Figure 3.3. The conditions for the GC are shown in Appendix A1. The column of the GC was a capillary column (EC-wax) connecting with FID detector. After that mixed xylenes, 1:1:1, was injected at the top of this cell. The membrane separation was carried out at a temperature of 140 °C, carrier gas flow rate of 5 ml/min. Figure 4.20 (D) shows the chromatogram of the permeates. The retention times of p- and m-xylenes, and o-xylene were 7.7 min. and 9.2 min., respectively. Reference peaks are shown in Figure 4.20 (A-C). From the analysis of the permeates by GC and comparison to the reference samples of the three isomers of xylenes, it showed that no separation took place. However, it was noticed that there was no pressure drop across the cell which was quite unusual for separation over a dense membrane. In addition, it could be seen that there was a gap between the silicalite membrane on the support and

the glass wall. Therefore, it is possible that the seal leaked which leads to permeation of all isomers as observed in the chromatogram, Figure 4.20 (D).

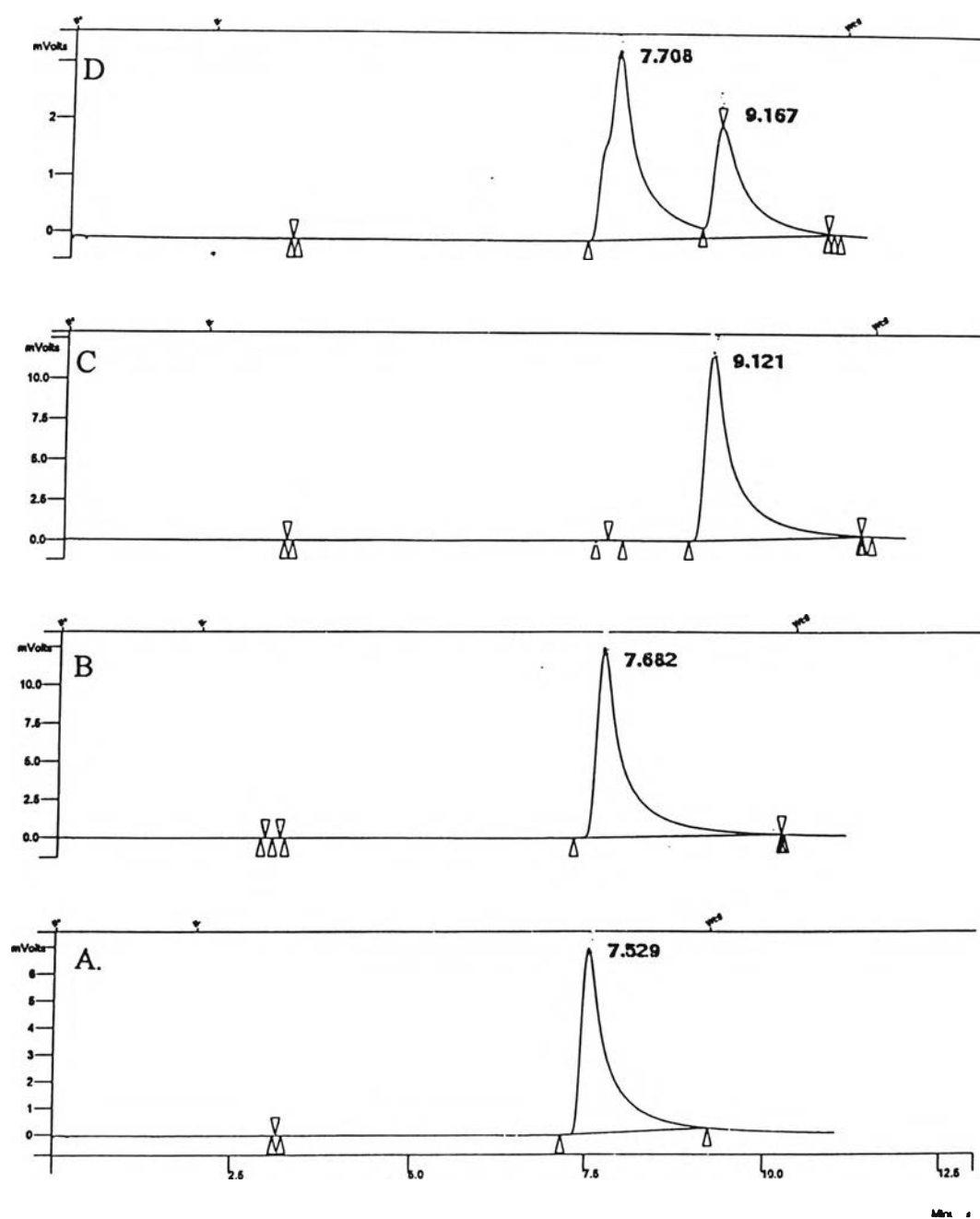


Figure 4.20 The gas chromatograms of xylene isomers and mixed xylenes diffusing through silicalite membrane at a temperature of 140 °C. The flow rate of carrier gas was 5 ml/min. A: p-xylene, B: m-xylene, C: o-xylene, D: mixed xylenes 1:1:1 (p-xylene : m-xylene : o-xylene). The column of GC was capillary column.

The sealing problem was solved by using epoxy resin as a binder. It was found that the cell sealed by epoxy resin, Figure 3.2 (B), generated a pressure drop of approximately 1 bar. The column and conditions for the GC were the same as those used for the cell sealed by gas welding. The membrane separation was again carried out at a temperature of 140 °C with a carrier gas pressure of 1 bar. p-xylene was injected to the top of the cell. Figure 4.21 (A) shows the peak of p-xylene which had the retention time at 7.5 min. After 1 hour, o-xylene was injected to the top of cell. Figure 4.21 (B) shows the result of permeates. It was found that only the peak of p-xylene was detected and no o-xylene was found. It is clear that the cell sealed by epoxy resin is applicable for testing the separation of mixed xylenes. The silicalite membrane showed high efficiency in separation of p-xylene from p- and o-xylenes mixture.

4.4.2 GC packed column

Although, it appeared that the silicalite membrane could separate p- and o-xylenes, the retention times of the samples obtained by using the capillary column were not constant. It might be because of the unstable pressure and flow rate of the carrier gas inside the column when the loop of gas sampling valve opened to fill the gas sample. This is because the capillary column is very small in diameter and the flow rate of the carrier gas was too low. Thus it was the limit of the capillary column for this case. Therefore, the packed column (carbowax) connecting with TCD detector was used instead of the capillary column to solve the problem of unstable retention time. The condition of GC for a carbowax packed column was shown in Appendix A2.

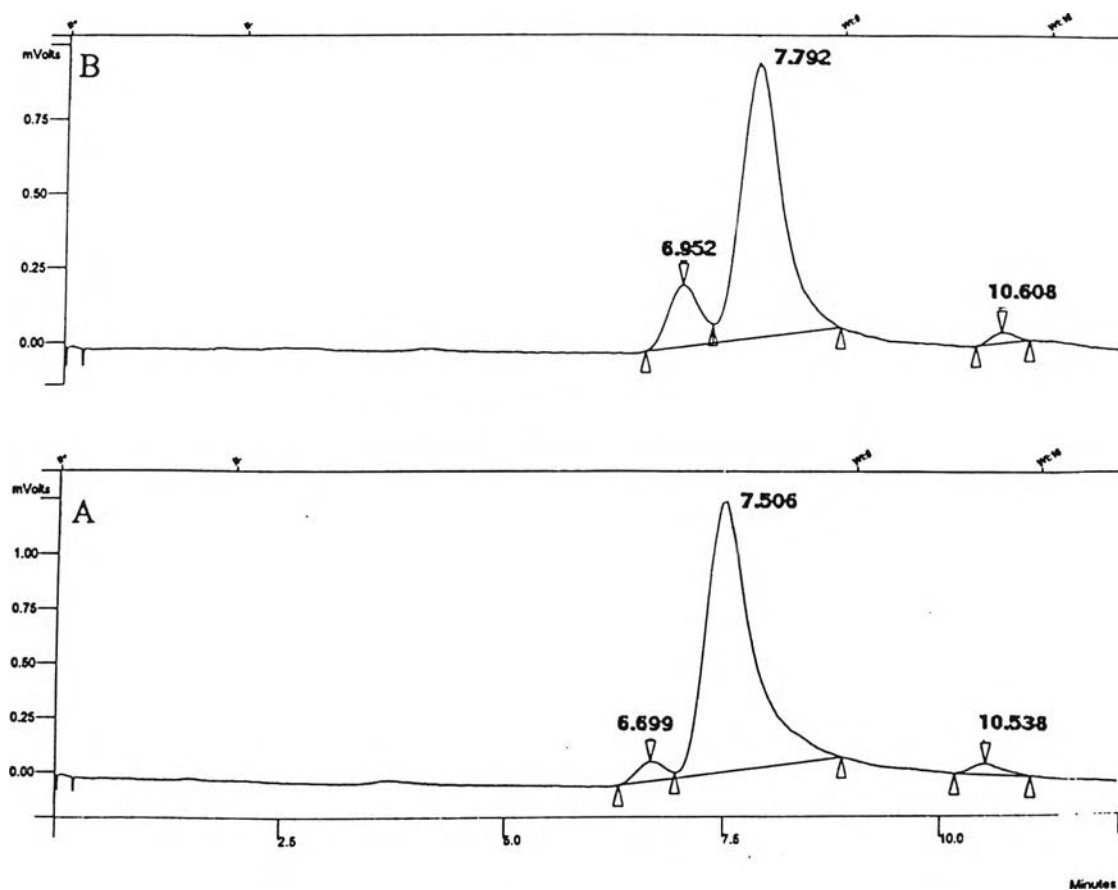


Figure 4.21 The gas chromatograms of mixed xylenes diffusing through silicalite membrane at a temperature of 140 °C, carrier gas pressure of 1 bar. A: p-xylene, B: mixed p-xylene and o-xylene.

The ratios of p-xylene : m-xylene : o-xylene in the standard samples of mixed xylenes used in the experiments were 1:1:1, 1:2:1 and 1:1:2 (wt. %). Figure 4.22 shows the gas chromatograms of mixed xylenes, 0.2 μL , injected, at the injection port with different weight ratios. The retention time of p-xylene was 9.5 min. The retention time of m-xylene was 9.8 min. (1:1:2) and 10.0 min. (1:2:1), and the retention time of o-xylene was 12.6 min. (1:2:1) and 13.1 min. (1:1:2). All peaks in Figure 4.22 were overlapped. Figure 4.23 shows the gas chromatogram of mixed xylenes (1:1:1), 0.06 μL , which injected at the injection port. It was found that the retention times of p-xylene, m-xylene and o-xylene were 8.9, 9.2 and 11.9 min., respectively. The peaks in Figure 4.22 (A) had longer retention time and broader than the peaks in Figure 4.23. Therefore, the best quantity of sample injection was 0.06 μL .

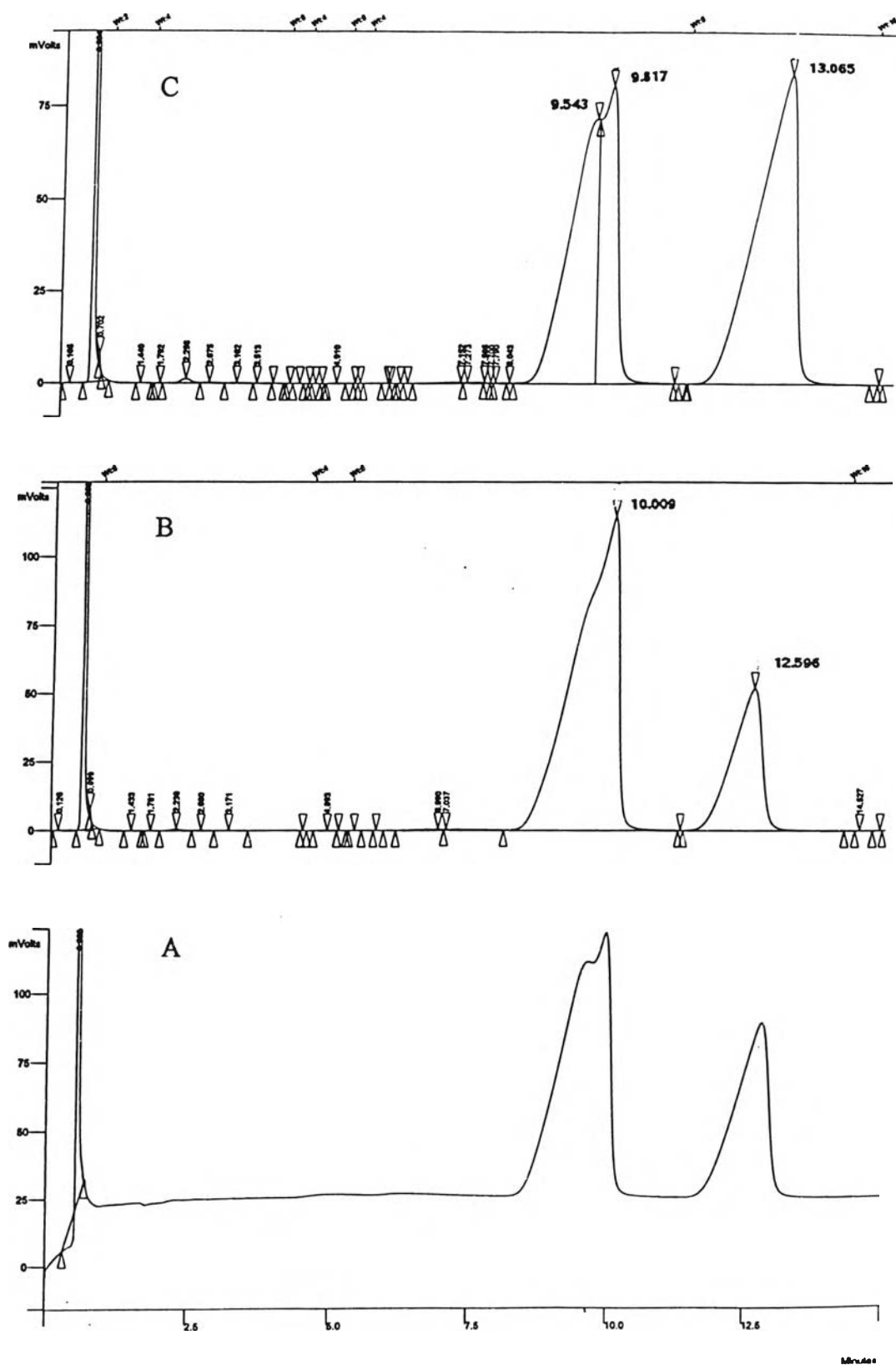


Figure 4.22 The gas chromatograms of mixed xylenes injected at injection port. A: 1:1:1, B: 1:2:1, C: 1:1:2 (p-xylene : m-xylene : o-xylene).

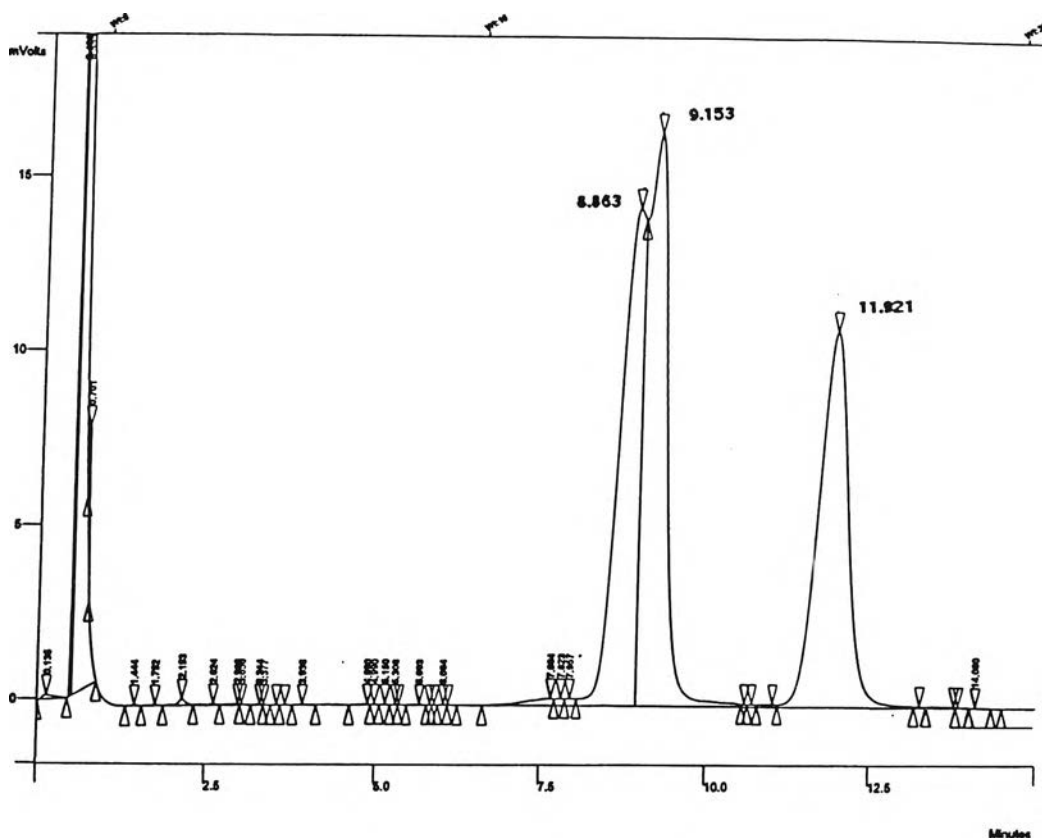


Figure 4.23 The gas chromatogram of mixed xylenes injected at the injection port (p-xylene : m-xylene : o-xylene = 1:1:1).

Figure 4.24 shows the gas chromatogram of mixed xylenes (1:1:1), 0.06 μL , injected through the loop of gas sampling valve. The retention times of p-xylene, m-xylene, and o-xylene were 8.8, 9.1 and 11.9 min., respectively, which were almost the same as those in Figure 4.23. Table 4.2 shows the comparison of retention time of each isomer. The retention times of the reference peaks in Figure 4.24 were used as the standard retention times in the experiments.

Table 4.2 The comparison of retention times of each isomer.

| Isomer | Injection at port (0.2 μL) | Injection at port (0.06 μL) | Injection through the loop of gas sampling valve (0.06 μL) |
|----------|---|--|---|
| p-xylene | 9.5 (1:1:2) | 8.9 | 8.8 |
| m-xylene | 9.8 (1:1:2) 10.0 (1:2:1) | 9.2 | 9.1 |
| o-xylene | 12.6 (1:2:1) 13.1 (1:1:2) | 11.9 | 11.9 |

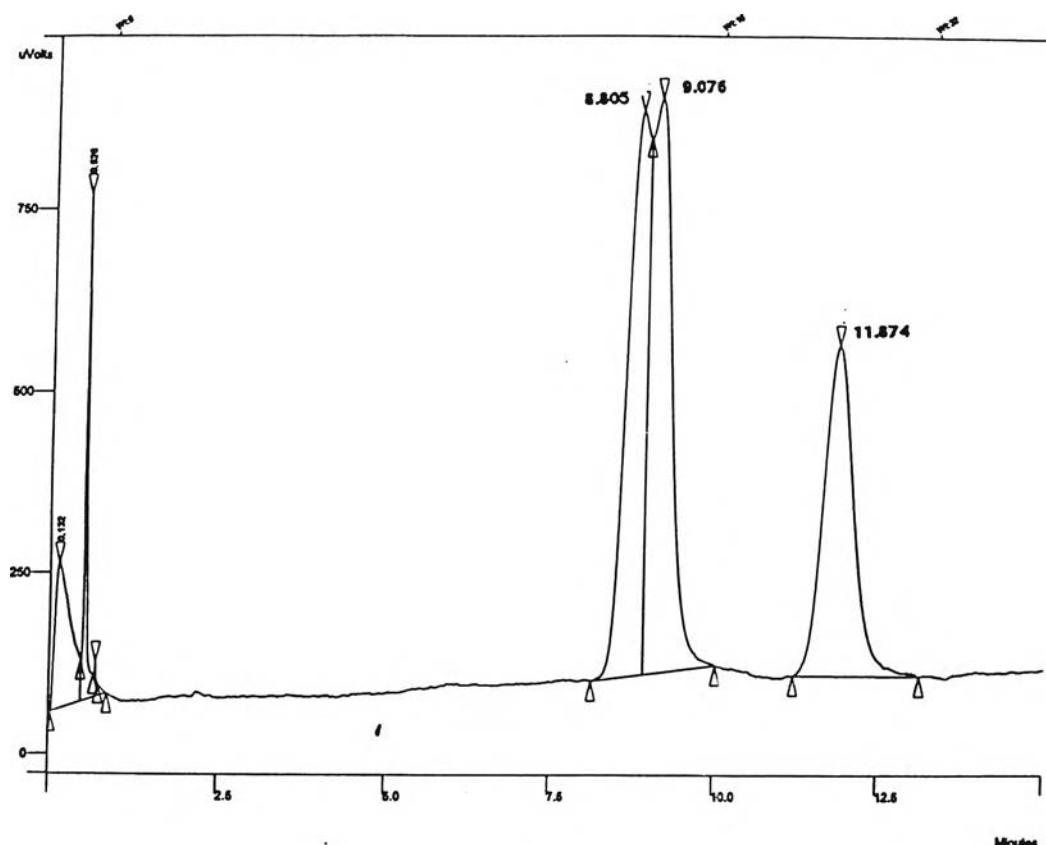


Figure 4.24 The gas chromatogram of mixed xylenes injected through the loop of gas sampling valve (p-xylene : m-xylene : o-xylene = 1:1:1).

Impurity

After the standard peaks were confirmed, the cell sealed by epoxy resin was installed with the gas sampling line. The membrane separation was carried out at a temperature of 140 °C, pressure of carrier gas 0.5 bar. Figure 4.25 (A) shows a chromatogram, before the installation of the cell with gas sampling line. No peak appeared. However, after the cell was installed, no sample was injected to the membrane, Figure 4.25 (B), a peak with the retention time of 5.8 min. was a peak of water. The result agreed with the retention time of water shown in Figure 4.26.

The peak of water is an impurity peak supposed to come from : the adsorption of water from the atmosphere by borosilicate disc support and silicalite membrane; and the elimination of water from the reaction of bisphenol A and epichlorohydrin during curing of epoxy resin [26]. The impurity peak of water was not observed in the experiment using the capillary column when FID detector was connected because FID detector will not detect water in the system.

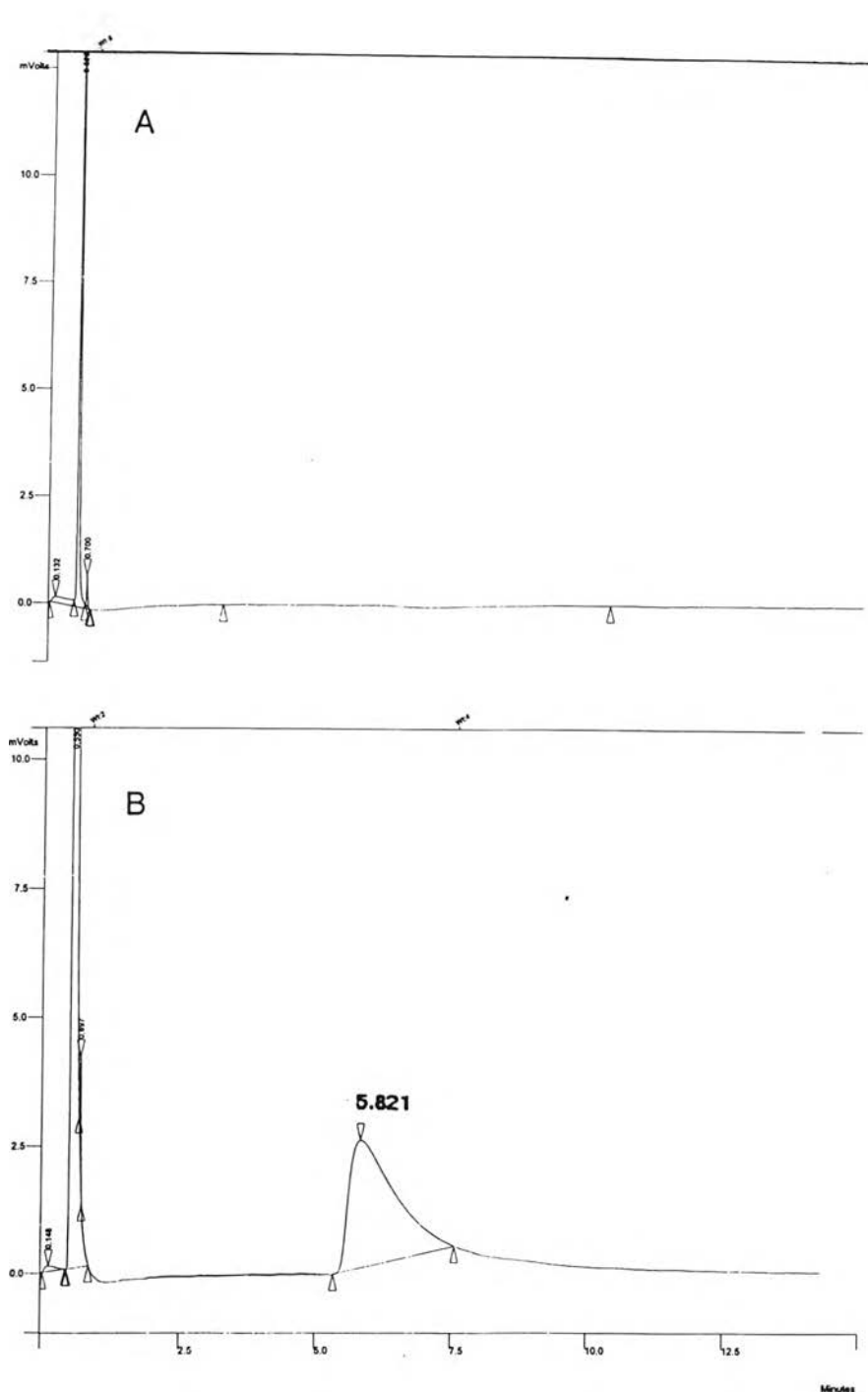


Figure 4.25 The chromatograms A: before the installation of the cell, B: after the installation of the cell.

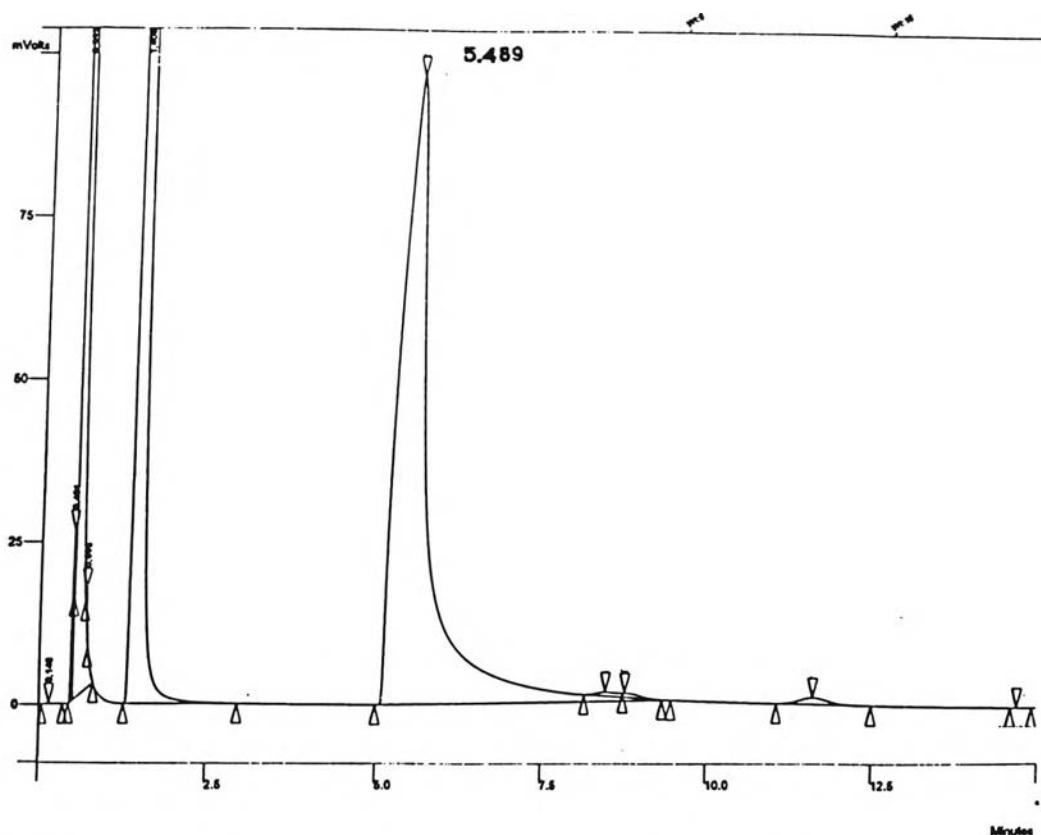


Figure 4.26 The chromatogram of water injected at injection port.

4.4.3 The separation with silicalite membrane

The separations of mixed xylenes were studied with different ratios of p-xylene : m-xylene : o-xylene as 1:1:1, 1:2:1 and 1:1:2. The cell was installed with the gas sampling line of GC. The separations were conducted at a temperature of 140 °C, pressure of carrier gas 0.5 bar. The injection was 0.5 μ L for each sample.

Figure 4.27 shows the gas chromatogram of mixed xylenes (1:1:1) diffusing through the silicalite membrane. It was found that the retention time of water was at 5.5 min. which overlapped with those of p- and m-xylenes (8.8 and 9.0 min.). Figure 4.28 shows the gas chromatogram of mixed xylenes (1:2:1) diffusing through the silicalite membrane. The result was almost the same as shown in Figure 4.27.

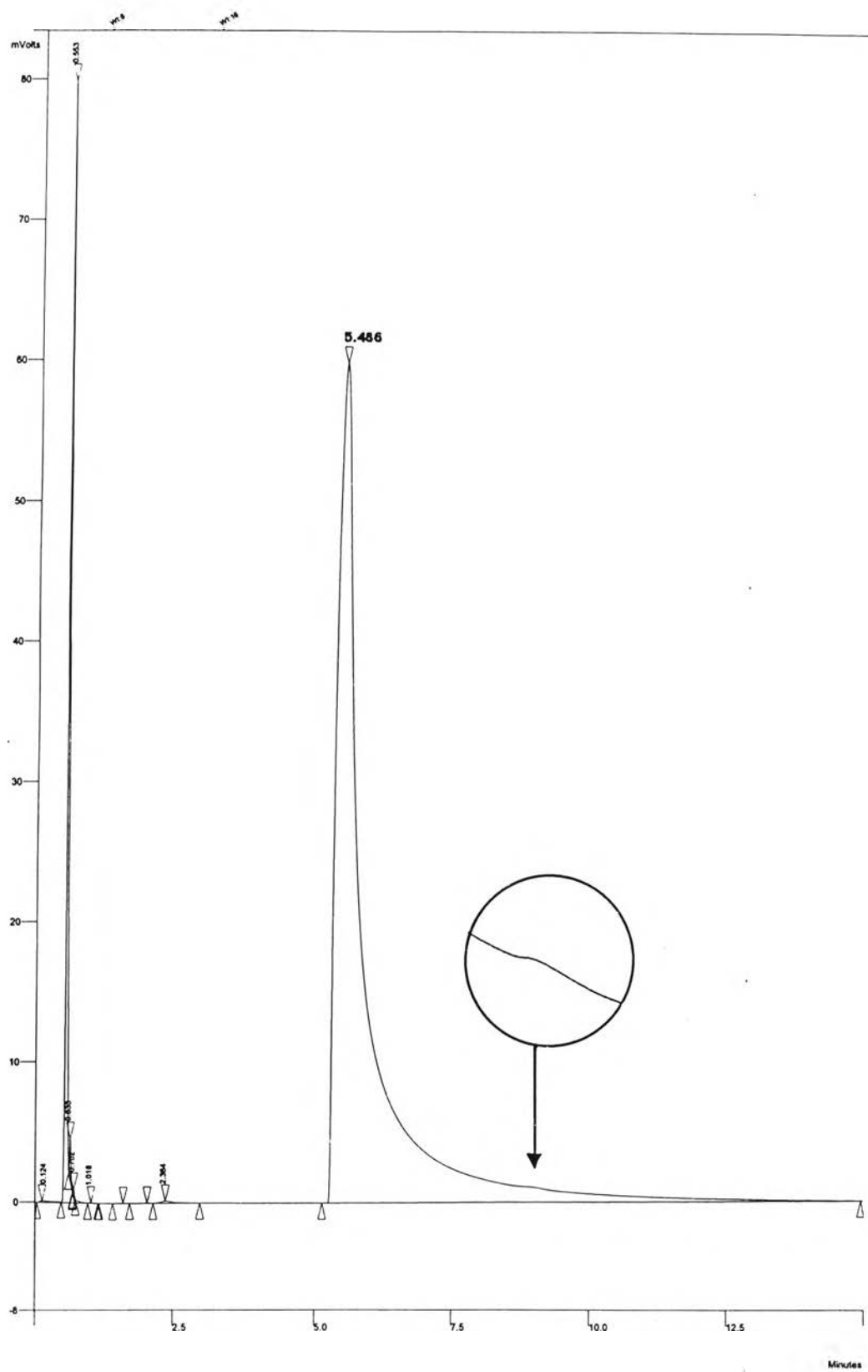


Figure 4.27 The gas chromatogram of mixed xylenes (1:1:1) diffusing through the silicalite membrane.

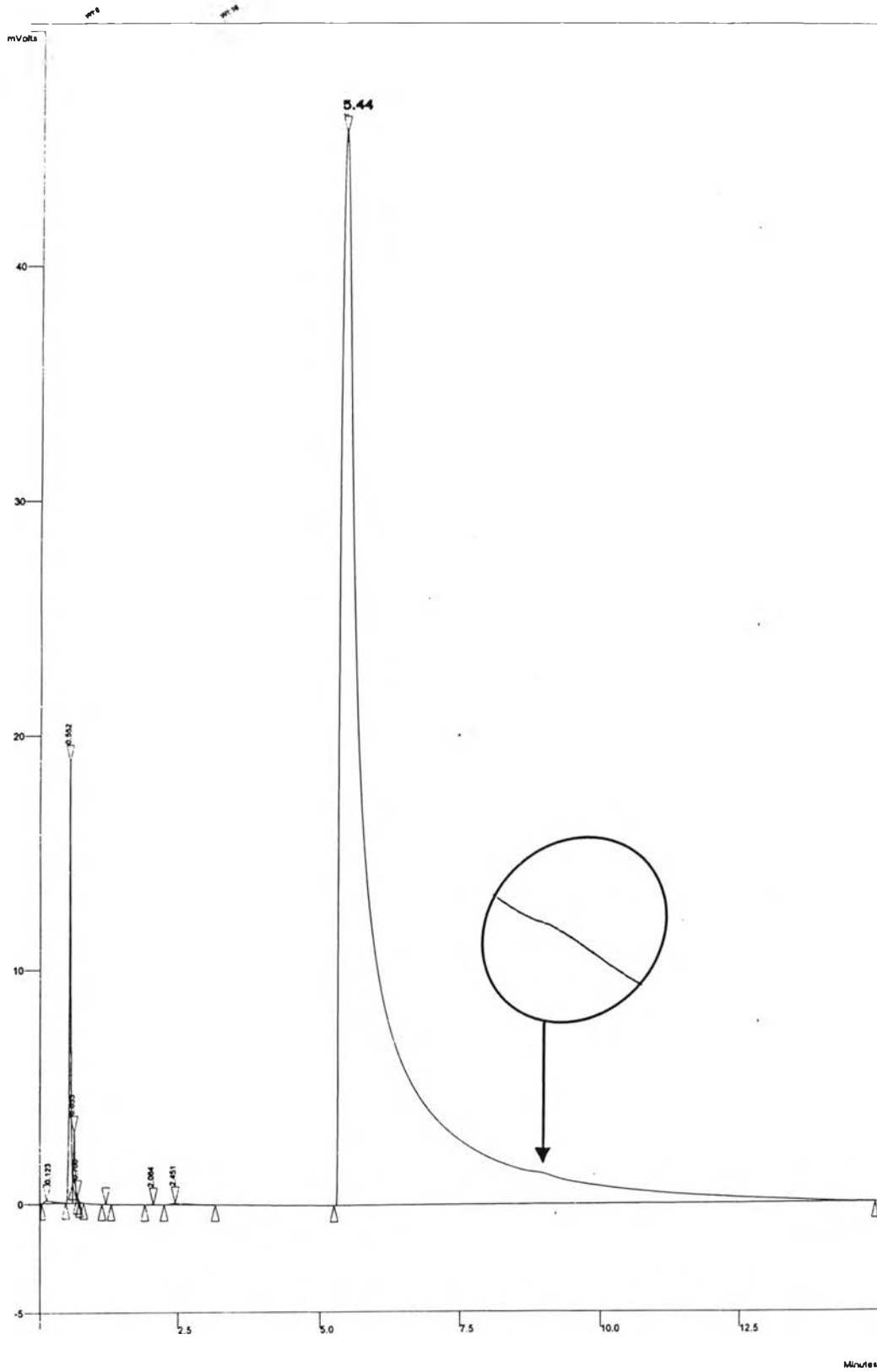


Figure 4.28 The gas chromatogram of mixed xylenes (1:2:1) diffusing through the silicalite membrane.

Comparing Figures 4.27, 4.28 and 4.24, it was shown that there was no peak at retention time of 11-12 min. which expected that o-xylene did not diffuse through the membrane. p-xylene and m-xylene diffused through the membrane at the retention time of 8.8-9.0 min.

The results of the separation of xylene isomers using TCD detector were not clear enough since there was an interference from peak of the water. To solve this interference FID detector was replaced. Figure 4.29 shows the gas chromatogram of mixed xylenes (1:1:1) diffusing through the silicalite membrane. It was found that the peak of p- and m-xylenes, and o-xylene appeared at the retention times of 9.0 and 11.9 min., respectively.

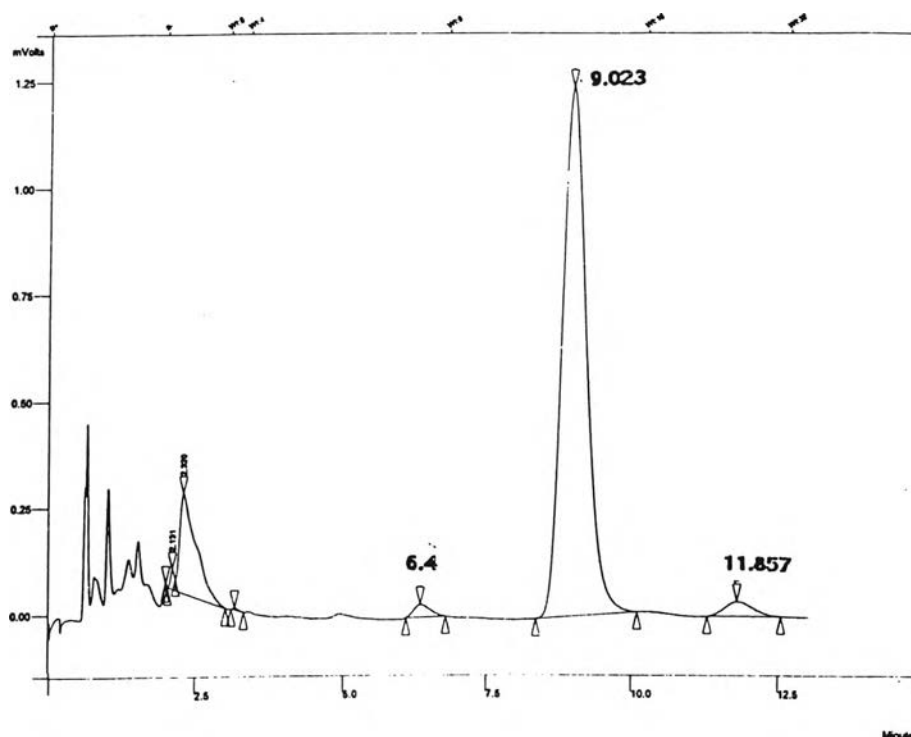


Figure 4.29 The gas chromatogram of mixed xylenes (1:1:1) diffusing through the silicalite membrane.

From Figure 4.29 showed that p- and m-xylenes can be selectively separated from o-xylene in mixed xylenes. The quantities of the permeates were different upon period of permeation. Table 4.3 shows the separation factor and permeate distribution

of p-, m- and o-xylenes. The calculation of these values were shown in Appendix A3. Equations are as follows:

$$\text{Separation factor } (\alpha) = \frac{\text{Chromatogram area fraction of permeate}}{\text{Chromatogram area fraction of feed}} \quad (4.1)$$

$$\text{Permeate distribution} = \frac{\text{Chromatogram area of permeate}}{\text{Chromatogram area of all permeates}} \quad (4.2)$$

Figure 4.30 shows the relation of permeation time and the separation factor. The separation factor of p- and m-xylenes reached a maximum value, 1.47, at 3 hours of permeation time. The separation factor of o-xylene decreased to a minimum value, 0.04, at 3 hours of permeation time. It is possible that p- and m-xylenes selectively diffuse into the pores and prevent the permeation of o-xylene. The averages of permeate distributions of p- and m-xylenes were 97.96 %, whereas, o-xylene was 2.04 %.

It is clear that the molecular size of p-xylene is close to pore size of the silicalite, therefore, p-xylene can easily diffuse through the silicalite membrane. Although m-xylene is relatively larger than p-xylene (Table 4.4) it can diffuse through the silicalite membrane. It can be explained that the diffusion phenomena in the silicalite membrane is in the range of configurational diffusion, see Figure 4.31. The diffusivity in the region of configurational diffusion depends on the sizes and configurations of the sorbate species [27]. The configuration of m-xylene might be matched with the pore size of the silicalite, therefore, m-xylene can diffuse through the silicalite membrane. Although the molecular size of o-xylene is equivalent to the molecular size of m-xylene, their configurations are different. The configuration of o-xylene cannot match with the pore size of the silicalite which leads to the difficulty in diffusion through the silicalite membrane.

Table 4.3 The separation factors and the permeate distributions of p-, m- and o-xylenes.

| Status | Time (min.) | Chromatogram area of p- and m-xylenes (mVolts x sec) | Chromatogram area of o-xylene (mVolts x sec) | Chromatogram area of mixed xylenes (mVolts x sec) | Separation factor of p- and m-xylenes | Separation factor of o-xylene | Permeate distribution of p- and m-xylenes (%) | Permeate distribution of o-xylene (%) |
|----------|----------------|---|---|--|---|-------------------------------------|--|--|
| Feed | | 1755 | 875 | 2630 | | | | |
| Permeate | 41 | 55.9 | 2.06 | 57.96 | 1.44 | 0.11 | 96.45 | 3.55 |
| | 73 | 36.1 | 1.16 | 37.26 | 1.45 | 0.09 | 96.89 | 3.11 |
| | 109 | 40.8 | 0.97 | 41.77 | 1.46 | 0.07 | 97.68 | 2.32 |
| | 141 | 51 | 0.72 | 51.72 | 1.47 | 0.04 | 98.61 | 1.39 |
| | 177 | 62.2 | 0.89 | 63.09 | 1.47 | 0.04 | 98.59 | 1.41 |
| | 208 | 50.2 | 0.83 | 51.03 | 1.47 | 0.04 | 98.37 | 1.63 |
| | 273 | 58.2 | 0.92 | 59.12 | 1.47 | 0.04 | 98.44 | 1.56 |
| | 316 | 35.1 | 0.47 | 35.57 | 1.47 | 0.04 | 98.68 | 1.32 |
| Total | | 389.5 | 8.02 | 397.52 | - | - | 783.71 | 16.29 |
| Average | | 48.69 | 1 | 49.69 | - | - | 97.96 | 2.04 |

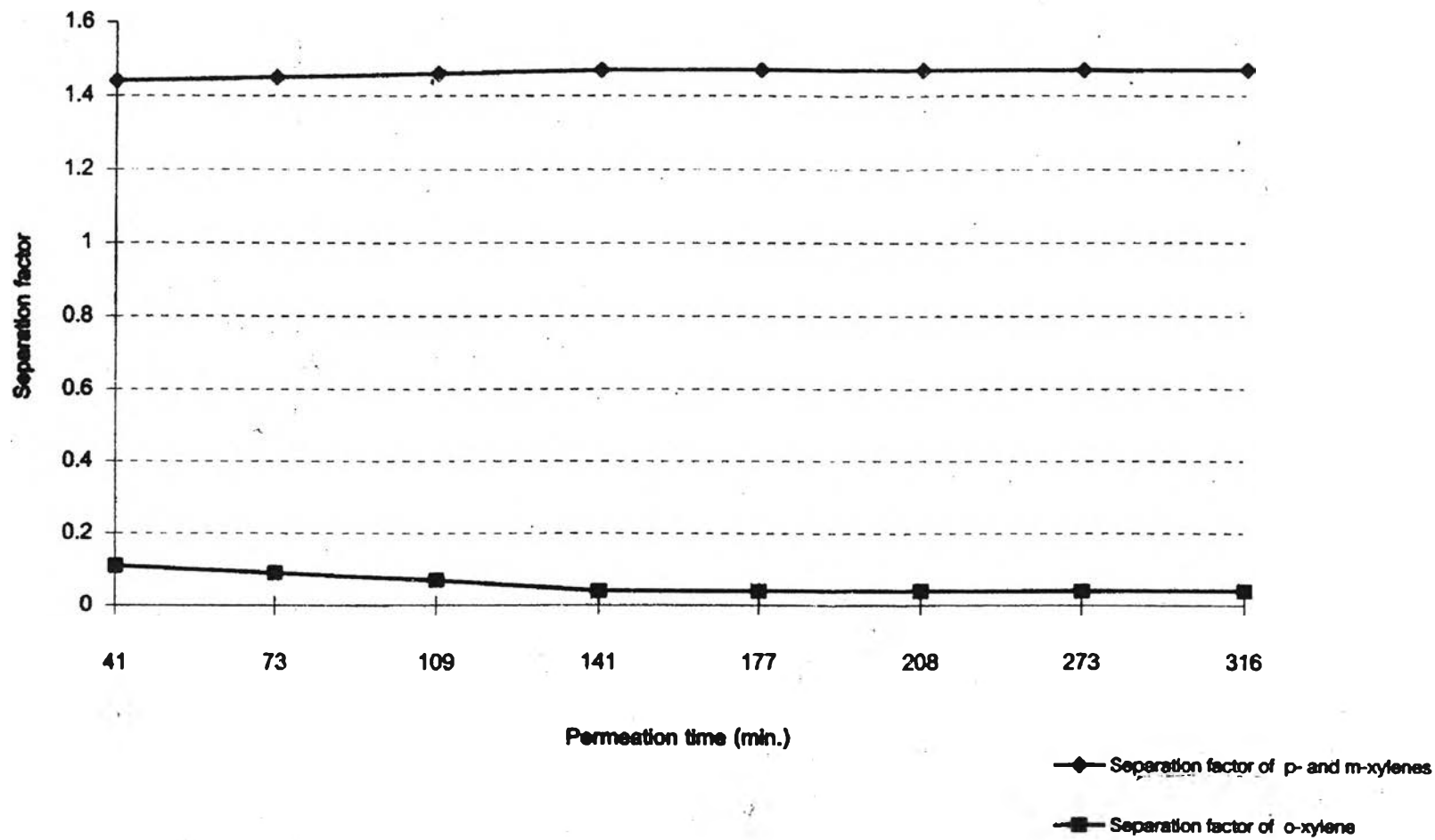

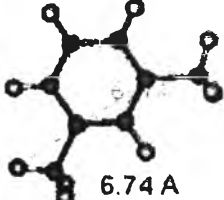
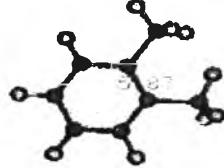
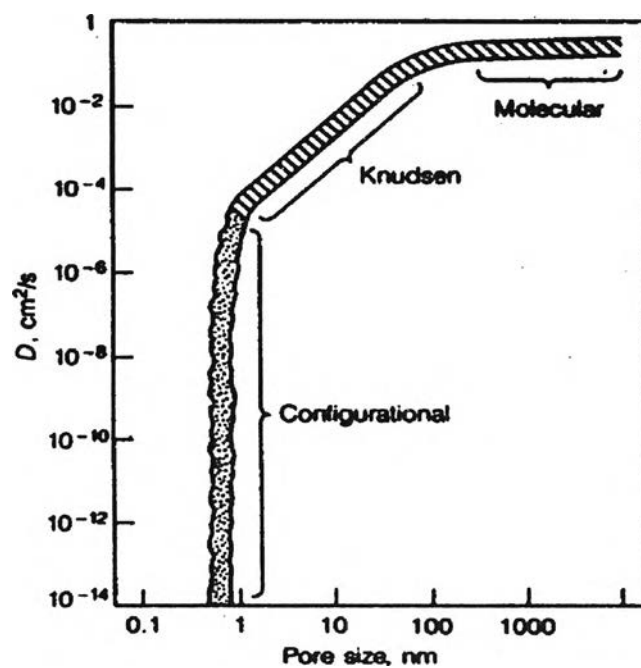


Figure 4.30 The relation between the permeation time and the separation factor.

Table 4.4 The kinetic diameters of xylenes [19].

| Sample | Kinetic diameter (nm.) | Molecular shape |
|----------|------------------------|---|
| p-xylene | 0.585 |  6.85 Å |
| m-xylene | 0.680 |  6.74 Å |
| o-xylene | 0.680 |  5.87 Å |

**Figure 4.31** Effect of pore size on molecular diffusivity in porous solid [27].

4.5 Crack of membrane

The membrane was cracked after use for 1-2 days. The membrane cannot be used for the separation of mixed xylenes as all isomers were detected at the retention times of 8.8-9.0 min. and 11.9 min. for p-, m-xylenes, and o-xylene, respectively, as shown in Figure 4.32 (TCD detector). The result was almost the same as shown in Figure 4.33 (FID detector). The crack of the membrane was shown by SEM image, Figure 4.34.

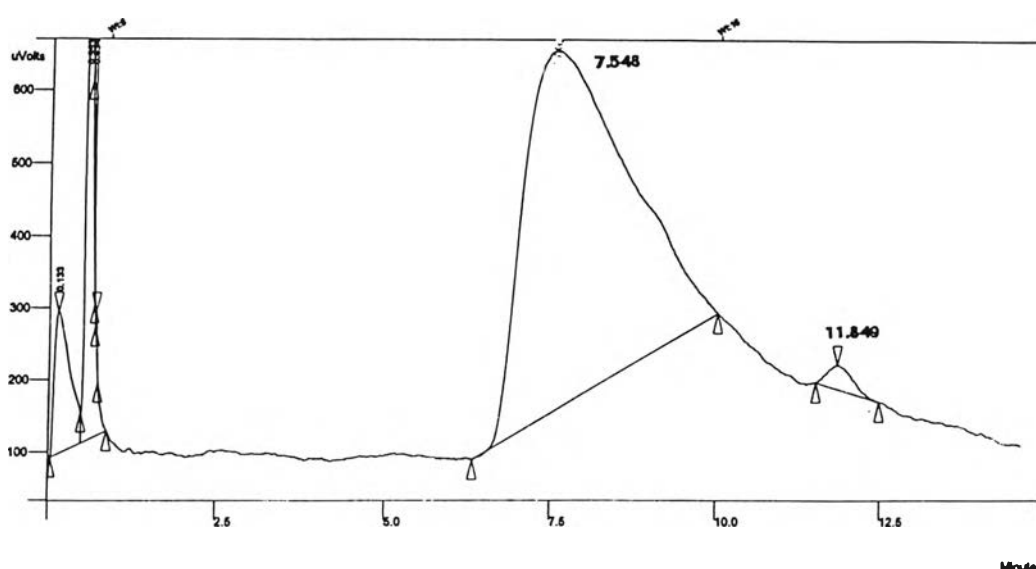


Figure 4.32 The gas chromatogram of mixed xylenes (1:1:2) diffusing through the silicalite membrane which crack occurred.

The crack of membrane might be caused by 2 main factors which were the shrinkage of epoxy resin and/or the use of over pressure of the carrier gas (≤ 1 bar). This is because the adhesive, epoxy resin, was used to seal between 3-way glass and the silicalite membrane and the shrinkage of epoxy resin occurred from curing which depended on temperature and time [26]. It was observed that the epoxy resin was changed the color from white to yellow. The amount of water resulting from curing of resin at the retention time of 5.4-5.5 min. decreased after using for 2 days, Figure 4.35.

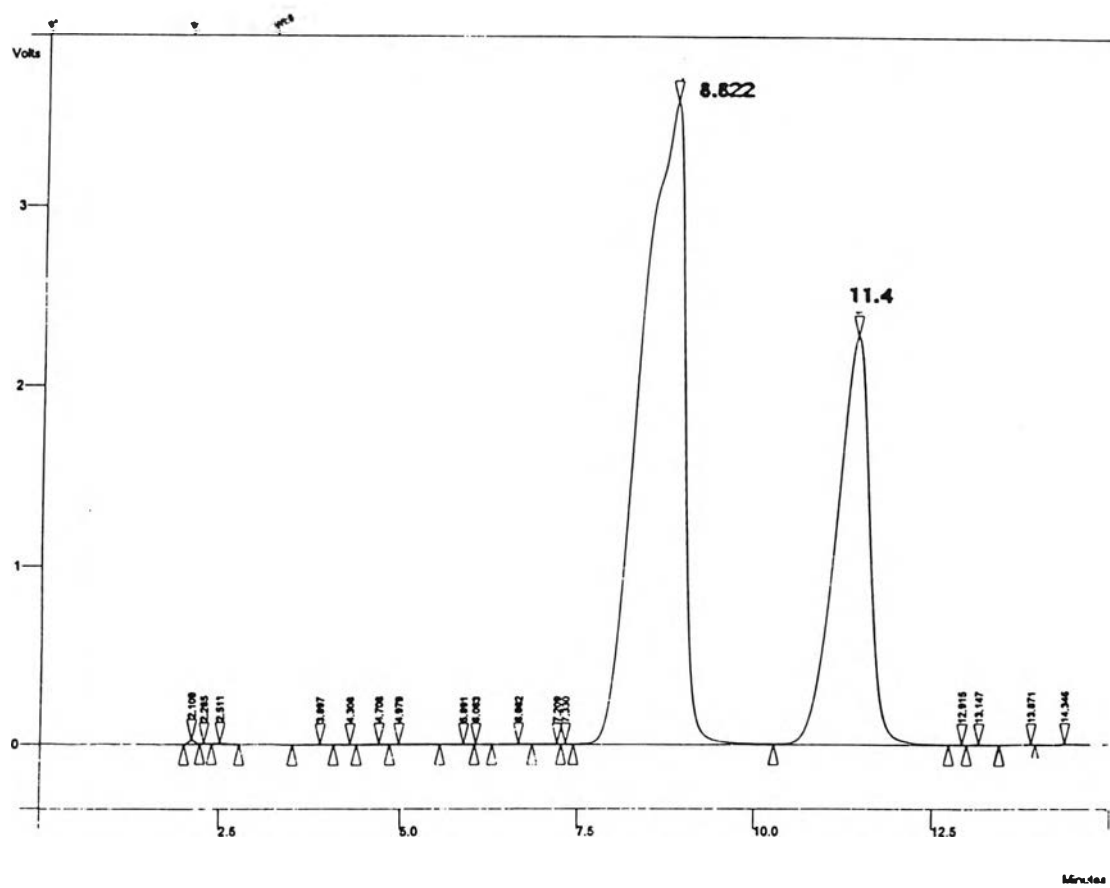


Figure 4.33 The gas chromatogram of mixed xylenes (1:1:1) diffusing through the silicalite membrane which crack occurred.

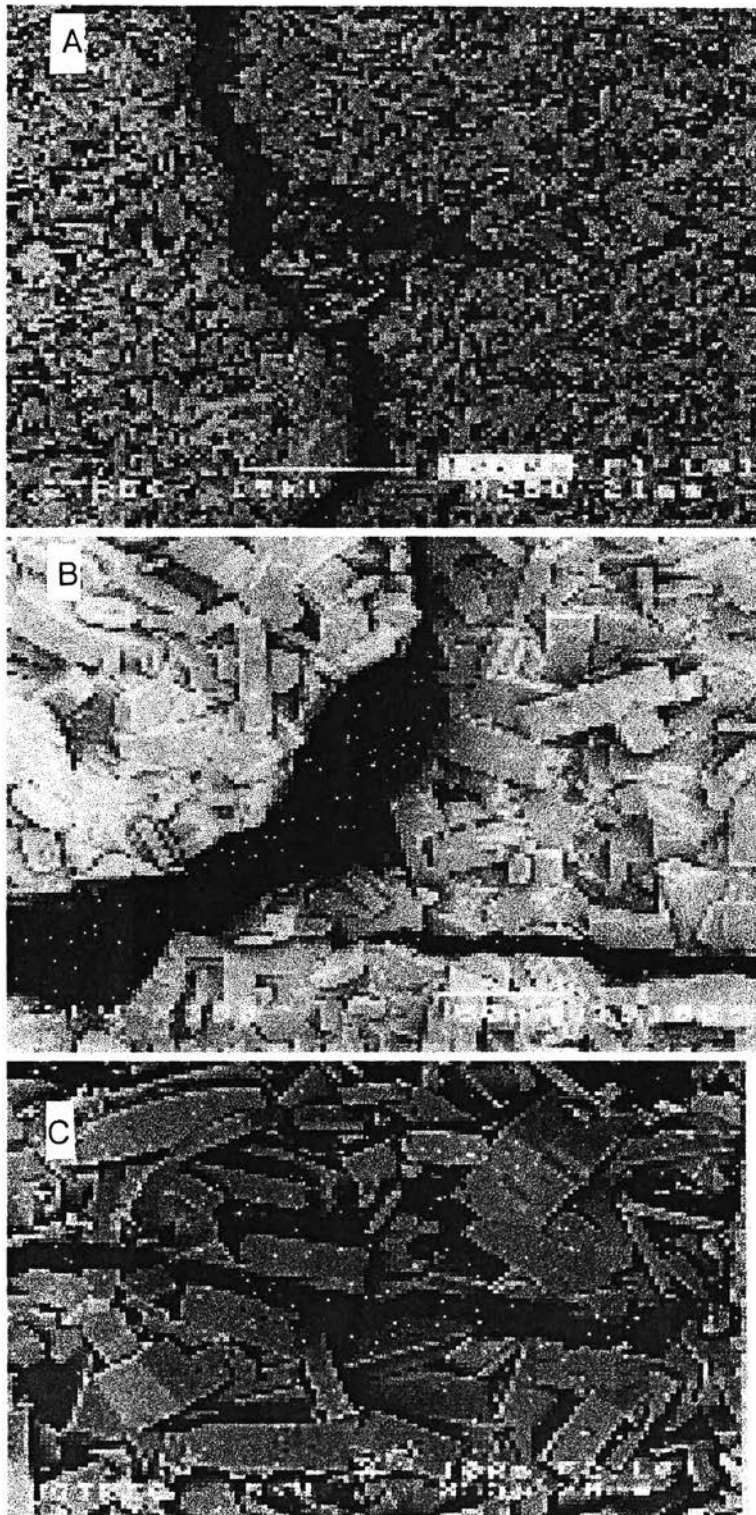


Figure 4.34 SEM images of crack of silicalite membrane. A: on support 4-5.5 μm ., B: on support 10-16 μm ., C: on support 16-40 μm .

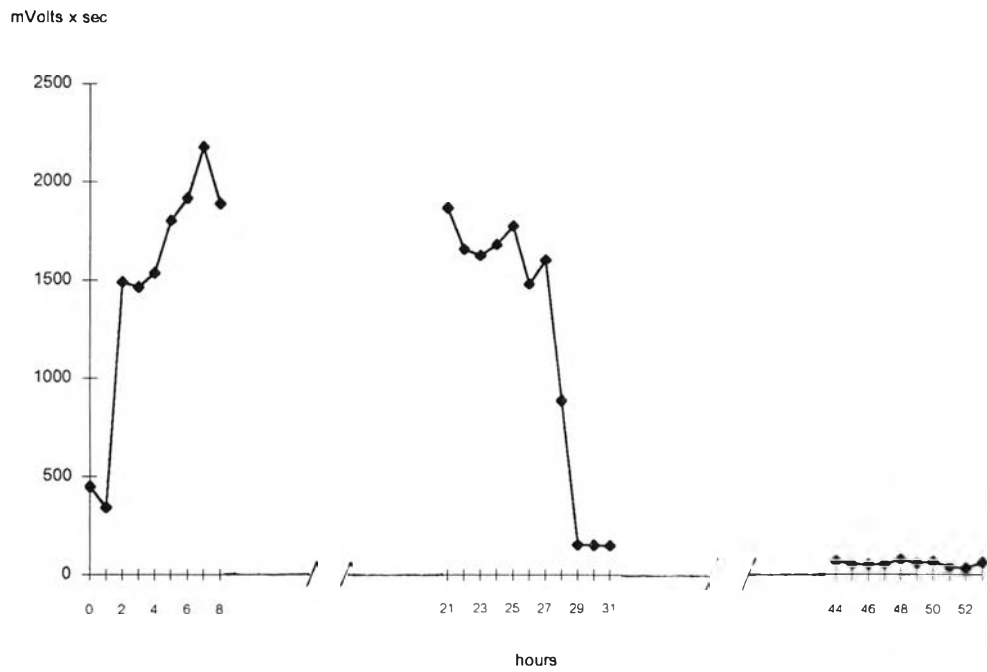


Figure 4.35 The chromatogram intensity of water was changed upon the curing time of resin.